JOURNAL OF GEOPHYSICAL RESEARCH, VOL. 105, NO. D5, PAGES 6785–6805, MARCH 16, 2000

Surface submicron aerosol chemical composition: What fraction is not sulfate?

P. K. Quinn,[1] T. S. Bates,[1] T. L. Miller,[2] D. J. Coffman,[2] J. E. Johnson,[2]
J. M. Harris,[3] J. A. Ogren,[3] G. Forbes,[4] T. L. Anderson,[5] D. S. Covert,[5] and M. J. Rood[6]

Abstract. Measurements of submicron aerosol mass and the mass of major ionic components have been made over the past 5 years on cruises in the Pacific and Southern Oceans and at monitoring stations across North America (Barrow, Alaska; Cheeka Peak, Washington; Bondville, Illinois; and Sable Island, Nova Scotia). Reported here are submicron concentrations of aerosol mass, nonsea salt (nss) sulfate, sea salt, methanesulfonate, other nss inorganic ions, and residual, or chemically unanalyzed, mass. Residual mass concentrations are based on the difference between simultaneously measured aerosol mass and the mass of the major ionic components. A standardized sampling protocol was used for all measurements making the data from each location directly comparable. For the Pacific and Southern Oceans, concentrations of the chemical components are presented in zonally averaged 20° latitude bins. For the monitoring stations, mean concentrations are presented for distinct air mass types (marine, clean continental, and polluted based on air mass back trajectories). In addition, percentile information for each chemical component is given to indicate the variability in the measured concentrations. Mean nss sulfate submicron aerosol mass fractions for the different latitude bins of the Pacific ranged from 0.14 ± 0.01 to 0.34 ± 0.03 (arithmetic mean ± absolute uncertainty at the 95% confidence level). The lowest average value occurred in the 40°–60°S latitude band where nss sulfate concentrations were low due to the remoteness from continental sources and sea salt concentrations were relatively high. Mean nss sulfate aerosol mass fractions were more variable at the monitoring stations ranging from 0.13 ± 0.004 to 0.65 ± 0.02. Highest values occurred in polluted air masses at Bondville and Sable Island. Sea salt mean mass fractions ranged between 0.20 ± 0.02 and 0.53 ± 0.03 at all latitude bands of the Pacific (except 20°–40°N where the residual mass fraction was relatively high) and at Barrow. The concentration of residual mass was significant at the 95% confidence level at all stations and all Pacific latitude bands (assuming that all errors were random and normally distributed and contamination of the samples did not occur beyond that accounted for by storage and transport uncertainties). Mean residual mass fractions ranged from 0.09 ± 0.07 to 0.74 ± 0.04.

1. Introduction

Tropospheric aerosols affect the Earth's radiation balance by scattering and/or absorbing a portion of the incoming solar radiation back to space [e.g., *Charlson et al.*, 1991]. Until the late 1990s, most model estimates as well as the Intergovernmental Panel on Climate Change (IPCC) [*IPCC,* 1996] summary of direct aerosol radiative forcing focused on a highly simplified anthropogenic sulfate-only aerosol. More recent estimates include other tropospheric chemical components such as sea salt, elemental carbon, organic carbon, and mineral dust [e.g., *Haywood et al.*, 1999, 1997; *Tegen et al.*, 1997; *Myhre et al.*, 1998]. These estimates suggest that nonsulfate components can have a significant impact. For example, model results of *Haywood et al.* [1999] indicate that sea salt is the leading aerosol contributor to the global-mean clear-sky radiation balance over oceans. In addition, the incorporation of nonsea salt (nss) sulfate into sea salt aerosol through gas/particle phase interactions leads to lower radiative forcing estimates than if the two chemical components are treated as separate particle populations [*Haywood*

[1]NOAA, Pacific Marine Environmental Laboratory, Seattle, Washington.
[2]Joint Institute for the Study of the Atmosphere and Ocean, University of Washington, Seattle.
[3]NOAA, Climate Monitoring and Diagnostics Laboratory, Boulder, Colorado.
[4]Environment Canada, Sable Island, Nova Scotia, Canada.
[5]Department of Atmospheric Sciences, University of Washington, Seattle.
[6]Department of Civil and Environmental Engineering, University of Illinois, Urbana-Champaign.

Paper number 1999JD901034.
0148-0227/00/1999JD901034$09.00

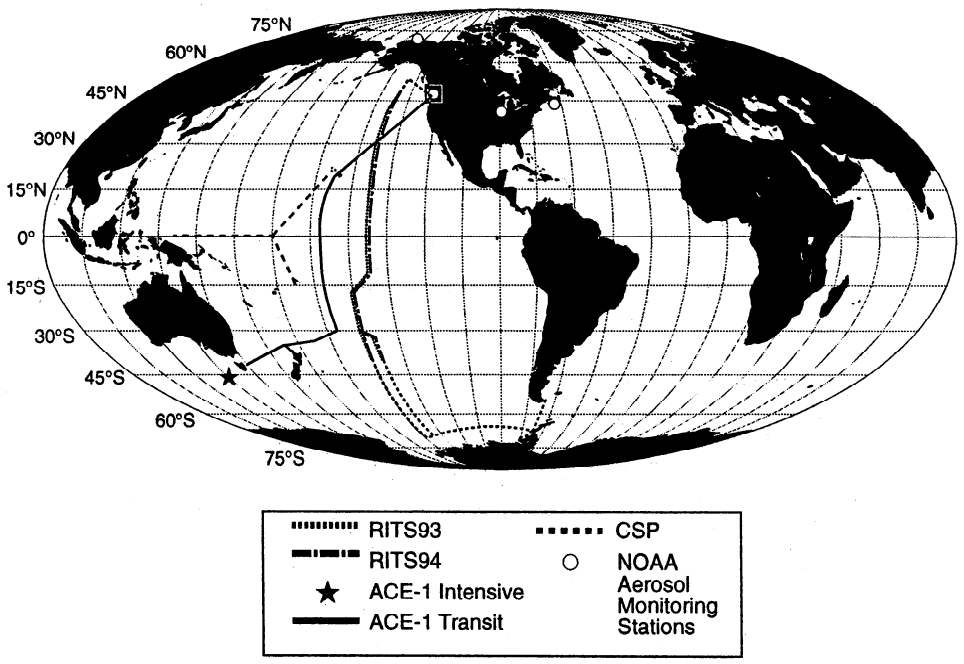

Figure 1. Cruise tracks through the Pacific (RITS 93, RITS 94, ACE 1, and CSP) (RITS, Radiatively Important Trace Species; ACE, Aerosol Characterization Experiment; CSP, Combined Sensor Program) and locations of aerosol sampling stations (Barrow, Alaska; Cheeka Peak, Washington; Bondville, Illinois; and Sable Island, Nova Scotia).

et al., 1999]. Clearly, model estimates of aerosol radiative forcing can be greatly improved by measurements that reveal the mass concentration of sulfate and nonsulfate aerosol components and the variability of these mass concentrations.

Simultaneous measurement of aerosol mass and the mass concentration of nss sulfate aerosol allows for a determination of the relative amounts of sulfate and nonsulfate aerosol components. During the past 5 years, these parameters have been measured on cruises in the Pacific and Southern Oceans and at a network of ground-level Northern Hemisphere monitoring stations. A standardized sampling and analysis protocol was used at all locations, resulting in the collection of comparable data over a wide range of geographical regions. In addition, the protocol allowed for a rigorous error analysis such that within the assumptions discussed in Section 2.5, uncertainties could be calculated at the 95% confidence level.

The cruises encountered air mass types ranging from remote to anthropogenically or continentally perturbed marine (see Figure 1 for cruise tracks and Table 1 for dates). The monitoring stations (National Oceanic and Atmospheric Administration (NOAA) Northern Hemi-

Table 1. Location and Dates for Cruise and Station Measurements

Experiment	Region	Date
RITS 93	Central Pacific (140°W, 55°N to 70°S)	March–May 1993
RITS 94	Central Pacific (140°W, 55°N to 70°S)	Nov. 1993 to Jan. 1994
ACE 1 Transit	Pacific (140°W to 172°E, 48°N to 43°S)	Oct.–Nov. 1995
ACE 1 Intensive	Southern Ocean (40° to 55°S, 135° to 160°E)	Nov.–Dec. 1995
CSP	Tropical Pacific (160°W to 140°E, 20°S to 20°N)	March–April 1996
Barrow	71.3°N, 156.6°W	Oct. 1997 to June 1998
Cheeka Peak	48.3°N, 124.6°W	March 1994 to Nov. 1995
Bondville	40.05°N, 88.4°W	Jan. 1996 to Dec. 1997
Sable Island	43.93°N, 60.0°W	Jan. 1996 to Dec. 1997

sphere regional monitoring sites) are located in the latitude band where models predict the largest sulfate aerosol radiative forcings downwind of industrial sources [*Charlson et al.,* 1991]. Cheeka Peak, Washington (48.3°N, 124.6°W, 480 m asl), is a coastal marine site located upwind of North America, Sable Island, Nova Scotia (43.9°N, 60°W, 5 m asl), is a marine site located downwind of North America, and Bondville, Illinois (40°N, 88.4°W, 230 m asl), is a continental site located in the Midwest United States in east-central Illinois. In addition, measurements have been made at Barrow, Alaska (71.3°N, 156.6°W, 8 m asl), an Arctic site that, depending on the time of year, is exposed to Arctic haze or remote marine air.

Presented here are submicron concentrations (aerodynamic particle diameter, $D_{aero} < 1.0$ μm at 30 to 45% RH) of aerosol mass and the dominant ionic chemical components: nss sulfate aerosol, sea salt, methanesulfonate (MSA^-), and other nss inorganic ions. Understanding the contribution of sulfur emissions to aerosol mass requires knowing the concentration of nss $SO_4^=$ ion and the mass of associated species [*Charlson et al.,* 1999]. Therefore nss sulfate aerosol as defined here includes both nss $SO_4^=$ and NH_4^+. Other nss inorganic ions include nss K^+, Mg^{+2}, Ca^{+2}, Cl^-, and Br^-; NO_3^-, and NH_4^+ in excess of an NH_4^+ to nss $SO_4^=$ molar ratio of 2. In addition, the residual, or chemically unanalyzed, mass concentration is determined from the difference between the aerosol mass and the mass of the ionic chemical components and their associated water. The focus is on submicron aerosol as this is the size range most efficient at scattering and absorbing incoming solar radiation.

2. Measurements

2.1. Aerosol Collection

During the Radiatively Important Trace Species cruises (RITS 93 and RITS 94), submicron aerosol samples were collected on 47 mm 1.0 μm Millipore Fluoropore filters with a cyclone upstream designed to remove particles with $D_{aero} > 1.0$ μm at the sampling flow rate of 50 standard liters per minute (sLpm). Samples were collected over a 3-day period. During the first Aerosol Characterization Experiment (ACE 1) and the Combined Sensor Program (CSP), samples were collected with two-stage Berner type multijet cascade impactors [*Berner et al.,* 1979] having 50% aerodynamic cutoff diameters of 1.0 and 10 μm at the sampling flow rate of 30 sLpm. Samples were collected over a 24-hr period. At the monitoring stations, submicron aerosol samples were collected on 47 mm Millipore Fluoropore filters (1.0 μm pore size) with an impactor upstream with a 50% aerodynamic cutoff diameter of 1.0 μm at the sampling flow rate of 30 sLpm. Samples were collected over a 24-hour period at Bondville and Sable Island and over the course of 1–5 days at Cheeka Peak and Barrow. The aerodynamic cutoff diameter of 1 μm (at the sampling reference RH of 30–45%) was chosen to completely collect the accumulation mode nss sulfate with minimal collection of coarse mode sea salt [see, e.g., *Quinn et al.,* 1996].

On all cruises and at all stations the dichotomous samplers described above were used to obtain concentrations of submicron aerosol mass, and the dominant ionic chemical components from which the residual mass concentration was derived. These data were used to calculate the mean values shown in Tables 3 and 5. In addition, with the exception of RITS 93 and RITS 94, they were used to calculate the percentile information shown in Figures 2 and 3. For RITS 93 and RITS 94, seven-stage Berner type cascade impactors were used to calculate the percentile information. The seven-stage impactor samples were collected on a shorter timescale (24 versus 72 hours) than samples from the dichotomous sampler which resulted in less averaging of the chemical component concentrations.

All shipboard and station samples were collected through a sector controlled inlet such that particle count, wind speed, and wind direction were used to avoid local sources of contamination. In addition, all inlets were heated up to 10°C above the ambient temperature so that the sampled aerosol was at a constant reference RH of 30–45%. At Bondville the air stream was conditioned to 40°C or 40% RH, whichever occured first. This allows for constant size segregation in spite of variations in ambient RH. Further details about the shipboard aerosol inlet are reported by *Quinn et al.* [1998].

All filter handling was done in a glove box purged with air that had passed through a scrubber containing potassium carbonate and citric acid to remove SO_2 and NH_3. After collection, shipboard samples were stored double bagged until analysis at Pacific Marine Environmental Laboratory (PMEL) with the outer bag containing citric acid to prevent absorption of gas phase NH_3. Station samples were shipped to NOAA PMEL for analysis in sealed tubes. Shipboard blank levels were determined by loading the sampler and deploying it at the sampling site for the length of a typical sampling period without drawing any air through it. The blank procedure was the same for the stations except that air was pulled through the blank filter for 10 s.

2.2. Gravimetric Analysis

Filters were weighed in the laboratory at NOAA PMEL before and after sample collection with a Mettler UMT2 microbalance. The microbalance was housed in a glove box kept at 33 ± 3% RH. Constant RH was maintained by circulating air through a flat baffle box containing a saturated solution of $MgCl_2 \cdot 6H_2O$ and then through the glove box [*Young,* 1967; *McInnes et al.,* 1996; *Quinn and Coffman,* 1998]. Maintaining the glove box at a constant RH allows each sampled filter to come into equilibrium with the same vapor pressure of water, thus reducing experimental uncertainty

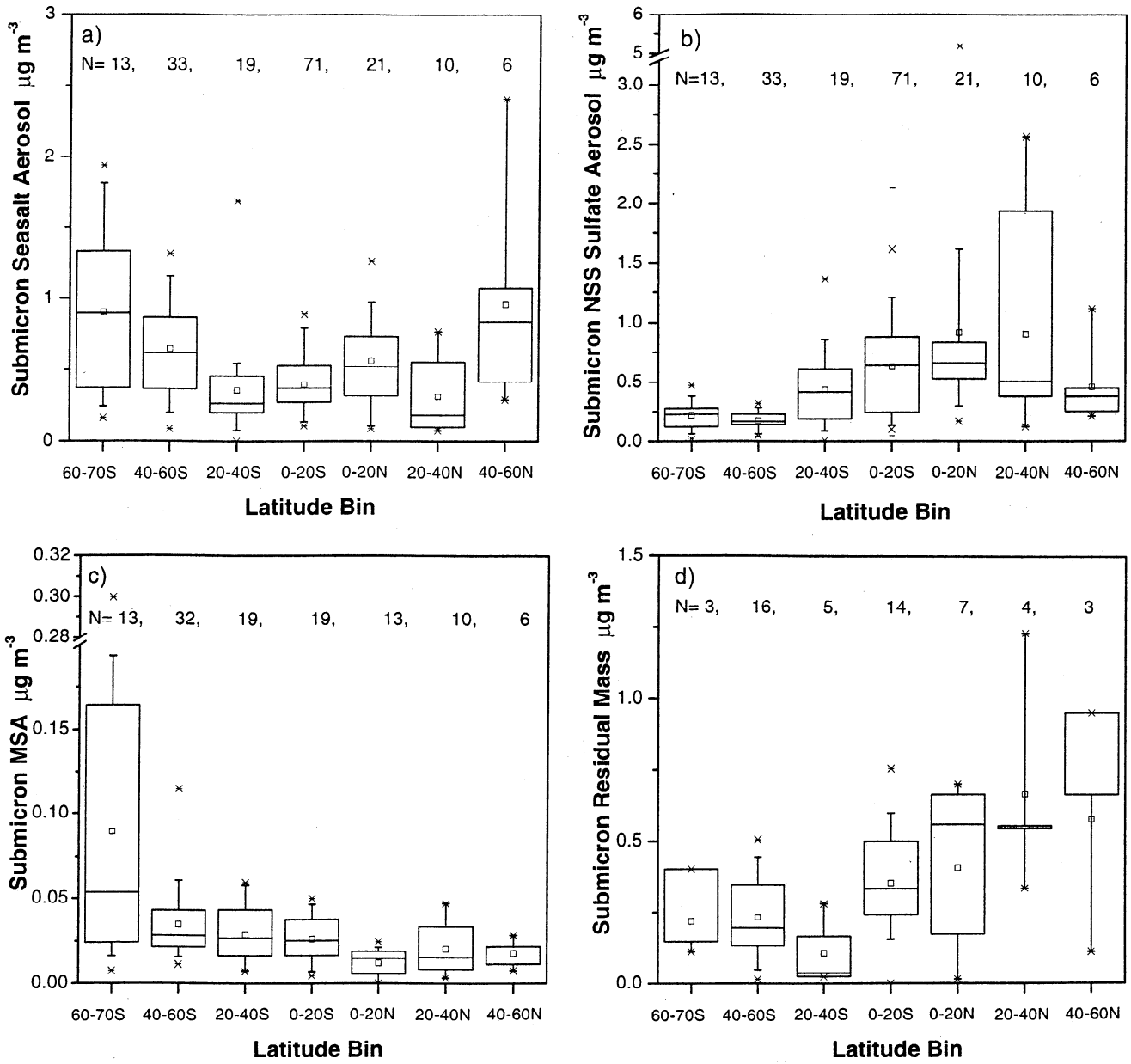

Figure 2. Box plots of submicron (a) sea salt, (b) nss sulfate aerosol (includes nss $SO_4^=$ and associated NH_4^+), (c) methanesulfonate, and (d) residual mass for latitude bins of the Pacific. Data from the four Pacific cruises were combined and then separated by latitude bin. The number of samples for each latitude bin, N, is shown at the top. The horizontal lines in the box denote the 25th, 50th, and 75th percentile values. The error bars denote the 5th and 95th percentile values. The two symbols below the 5th percentile error bar denote the 0th and 1st percentile values, and the two symbols above the 95th percentile error bar denote the 99th and 100th percentiles. The square symbol in the box denotes the mean.

due to a variable laboratory RH. The circulated air was cleaned by passing it through a scrubber containing activated charcoal, potassium carbonate, and citric acid. Substrates were equilibrated overnight in the glove box prior to weighing. Static charging, which can result in balance instabilities, was minimized by coating the walls of the glove box with a static dissipative polymer (Tech Spray, Inc.), placing an antistatic mat on the glove box floor, wearing antistatic gloves while handling the filters, and exposing the filters to a ^{210}Po source to dissipate any built-up charge. The reported submicron aerosol mass concentrations include the water mass that is associated with the aerosol on the filter at the glove box RH.

2.3. Ion Analysis

After the final weighing, filters were extracted and analyzed by ion chromatography for Na^+, NH_4^+, K^+, Mg^{+2}, Ca^{+2}, Cl^-, Br^-, NO_3^-, $SO_4^=$, and MSA^- [*Quinn et al.*, 1998]. With the exception of the Bondville site,

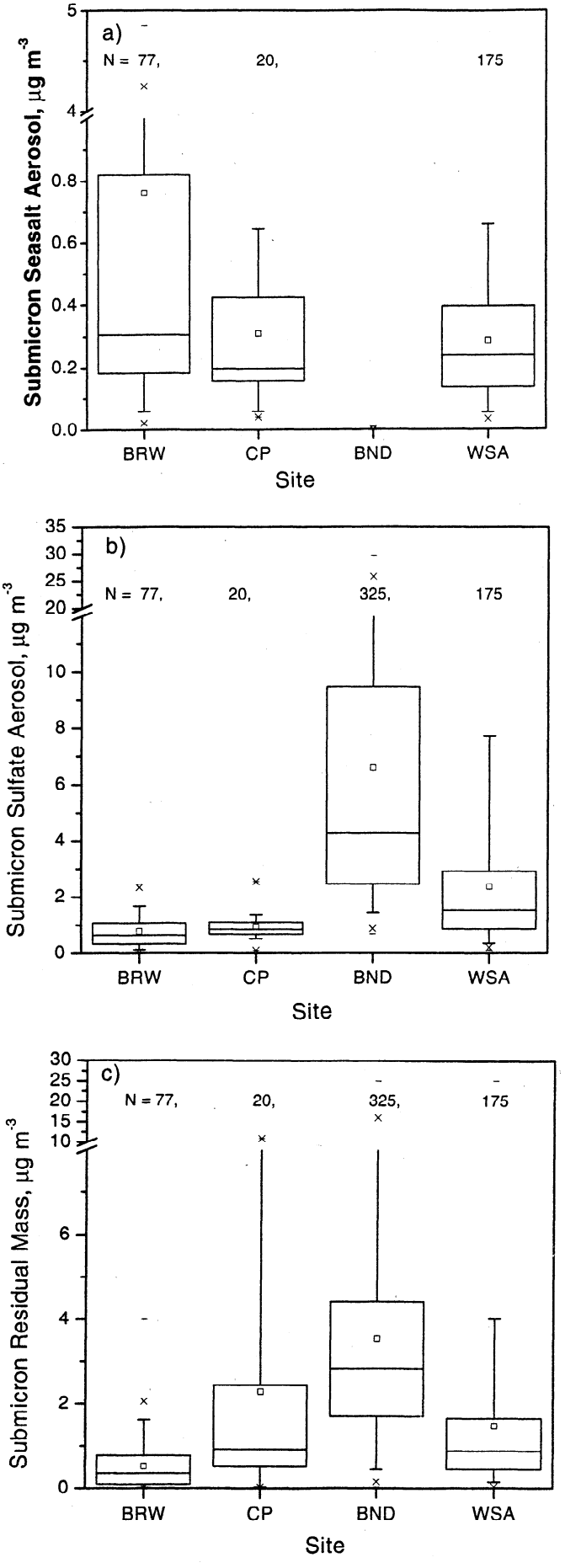

concentrations of nss K^+, Mg^{+2}, Ca^{+2}, Cl^-, and Br^- were calculated from the measured value and the seawater ratio of the ion to Na^+ assuming that all Na^+ was derived from sea salt. For the Bondville samples, all measured inorganic ions not associated with $SO_4^=$ aerosol (i.e., $SO_4^=$ and NH_4^+) were defined as "other inorganic ions."

2.4. Calculation of Water and Residual Mass

The water mass associated with nss $SO_4^=$ and sea salt aerosol at 33% RH was calculated using the measured ionic composition and the chemical thermodynamic equilibrium model AeRho [*Quinn and Coffman,* 1998]. In these calculations it is assumed that the aerosol is an external mixture of nss $SO_4^=$ aerosol (composed of nss $SO_4^=$, NH_4^+, and H_2O) and sea salt (composed of Na^+, Cl^-, sea salt $SO_4^=$, and H_2O) or, in the case of Bondville, sulfate aerosol and other inorganic ions. In this application, AeRho is a static model. It is designed to take the measured ionic composition of the aerosol and the constant sampling RH and determine the molecular composition of the chemical species within the aerosol. The molecular composition is then used to calculate the water mass associated with the aerosol. The model is not used to describe a dynamic system in which changes in the concentration of gas phase species affect the aerosol molecular composition. In addition, because of the constant sampling RH, it is not necessary to take into account changes in particle size with changes in RH.

The assumption of an external mixture may result in an overprediction of the water concentration (and hence an underestimation of the residual mass concentration) if the aerosol is internally mixed. This is because the assumption of an externally mixed aerosol precludes the reaction of nss $SO_4^=$ with sea salt Na^+ to form Na_2SO_4 or other hydrates that may form with Na^+–$SO_4^=$ mixtures [*Koloutsou-Vakakis and Rood,* 1994]. Since Na_2SO_4 crystallizes at an RH of 59% [*Tang et al.,* 1997], it is likely that it would be present as a solid which would result in a lower water mass concentration than that predicted from an external mixture [*Quinn and Coffman,* 1998].

Figure 3. Box plots of submicron (a) sea salt, (b) nss sulfate aerosol (includes nss $SO_4^=$ and associated NH_4^+), and (c) residual mass for Barrow, Alaska; Cheeka Peak, Washington; Bondville, Illinois; and Sable Island, Nova Scotia. The number of samples for each site, *N*, is shown at the top. The horizontal lines in the box denote the 25th, 50th, and 75th percentile values. The error bars denote the 5th and 95th percentile values. The two symbols below the 5th percentile error bar denote the 0th and 1st percentile values, and the two symbols above the 95th percentile error bar denote the 99th and 100th percentiles. The square symbol in the box denotes the mean.

Table 2. Sources of Uncertainty in the Determination of the Mass Concentration of Aerosol Chemical Components

Parameter	Sources of Uncertainty	Absolute Uncertainty	Overall Relative Uncertainty	Comments
Submicron aerosol mass concentration, M_g			±8.2%	M_g = 2.5 μg m^{-3}, m_g = 112.5 μg, V_a = 45 m^3
Δm_f, Δm_i	weighing	±4 μg/filter[a]		2σ of repetitive weighings of a sample filter
$\Delta(m_{f,b} - m_{i,b})$	storage and transport	±4 μg/filter[a]		2σ of initial and final weighings of blank filters
Δf(RH,ions)	glove box RH	±0.015[a,b]		based on f(RH,ions) of 1.025 and a chemical composition range of NH_4HSO_4 to $(NH_4)_2SO_4$
ΔV_a	air volume	±2.2 m^3		
Submicron aerosol ionic mass concentration, M_{IC}			±11%	M_{IC} = 1.5 μg m^{-3}, $\Sigma m_{\mathrm{ppm},j}$ = 12.4 μg mL^{-1}, $\Sigma m_{\mathrm{ppm\_}bj}$ = 1.1 μg mL^{-1}, V_l = 6 mL, m_{IC} = 67.8 μg, V_a = 45 m^3
$\Sigma(\Delta m_{\mathrm{ppm},j})$	IC analysis and filter extraction	±0.36 ppm[a]		2σ of repetitive analysis for ion j on a sample filter
$\Sigma(\Delta m_{\mathrm{ppm\_}b,j})$	IC analysis and filter extraction	±0.95 ppm[a]		2σ of repetitive analysis for ion j on a blank filter
ΔV_l	extract liquid volume	±0.2 mL		
ΔV_a	air volume	±2.2 m^3		
Submicron calculated aerosol water mass concentration, M_w			±8.0	M_w = 0.5 μg m^{-3}, m_w = 22.5 μg, V_a = 45 m^3
$\Delta m_{\mathrm{chem\_comp}}$	measured chemical composition	±1.2 μg/filter[a]		sensitivity of model output to range of uncertainty in measured chemical composition
$\Delta m_{\mathrm{RH\_T}}$	glove box RH and T	±0.67 μg/filter[a]		sensitivity of model output to range of uncertainty in glove box RH and T
ΔV_a	air volume	±2.2 m^3		
Submicron residual mass concentration, M_r			±53%	M_g = 2.5 μg m^{-3}, M_{IC} = 1.5 μg m^{-3}, M_w = 0.5 μg m^{-3}, M_r = 0.5 μg m^{-3}
ΔM_g	submicron aerosol mass	±0.20 μg m^{-3}		see above
ΔM_{IC}	submicron aerosol ionic mass	±0.16 μg m^{-3}		see above
ΔM_w	submicron calculated aerosol water mass	±0.04 μg m^{-3}		see above

Uncertainties are at the 95% Confidence Level. Concentrations of M_g, M_{IC}, M_w, and M_r and resulting relative uncertainties are for one case of marine aerosol (see comments). Relative uncertainties will be lower for the higher concentrations found in polluted atmospheres.

[a]For ACE 1. Absolute uncertainties vary with experiment.

[b]Assumes a chemical composition of NH_4HSO_4 [*McInnes et al.*, 1996].

The residual or chemically unanalyzed mass was estimated by subtracting the ionic mass plus the water mass associated with nss $SO_4^=$ and sea salt aerosol at 33% RH from the gravimetrically measured aerosol mass.

2.5. Uncertainty Analysis

Uncertainties associated with the determination of the aerosol, ionic, water, and residual mass were calculated as described in sections 2.5.1–2.5.4. It was assumed that all errors were random so that uncertainties were propagated as a quadratic sum of all errors involved (e.g., Wilson, 1952). Throughout the paper, Δ refers to absolute uncertainty at the 95% confidence level, and δ refers to relative uncertainty. The use of the 95% confidence level follows the recommendation of the National Institute of Standards and Technology (NIST) [*Taylor and Kuyatt*, 1994]. It is assumed that

the uncertainties are normally distributed so that dividing the uncertainties by 2 results in the 1σ values. The reported 95% confidence level applies to the average of the samples collected here, not to the average aerosol chemical composition for a given location. Absolute uncertainties for each source of uncertainty and overall relative uncertainties for the aerosol, ionic, water, and residual mass are given in Table 2 for concentrations typical of the marine atmosphere. Overall relative uncertainties will be lower for the higher concentrations found in polluted atmospheres.

2.5.1. Uncertainty of submicron aerosol mass. The amount of sampled material on the filter is

$$m_g = [(m_f - m_i) - (m_{f,b} - m_{i,b})] \quad (1)$$

in units of μg per filter. The m_i and $m_{i,b}$ are the initial masses of the sample and blank filters prior to exposure, and m_f and $m_{f,b}$ are the final masses of the sample and blank filters after exposure. The gravimetrically determined submicron aerosol mass concentration, M_g, in μg m^{-3} was calculated from

$$M_g = [((m_f - m_i) - (m_{f,b} - m_{i,b})) \cdot f(RH, \text{ions})] / V_a. \quad (2)$$

The $f(RH,\text{ions})$, which is equal to

$$f(RH, \text{ions}) = m_g(33\%\_RH)/m_g(\text{glove\_box}\_RH), \quad (3)$$

takes into account variations in water mass associated with material on the filter with deviations of the glove box humidity from 33%. V_a is the volume of air sampled in m^3 at 25°C and 1 atm.

The relative uncertainty of M_g, δM_g, was determined from

$$\delta M_g = \frac{\Delta M_g}{M_g} = \left[\left(\frac{\Delta m_g}{m_g}\right)^2 + \left(\frac{\Delta f(RH, \text{ions})}{f(RH, \text{ions})}\right)^2 + \left(\frac{\Delta V_a}{V_a}\right)^2\right]^{\frac{1}{2}}, \quad (4)$$

where the absolute uncertainty in m_g, Δm_g, is

$$\Delta m_g = \left[(\Delta m_f)^2 + (\Delta m_i)^2 + (\Delta (m_{f,b} - m_{i,b}))^2\right]^{\frac{1}{2}}. \quad (5)$$

2.5.2. Uncertainty of submicron ionic aerosol mass and individual ionic chemical components. Ionic aerosol mass concentration, M_{IC}, in units of μg m^{-3} was calculated from

$$M_{IC} = [\Sigma (m_{\text{ppm},j} - m_{\text{ppm\_b},j}) V_l] / V_a. \quad (6)$$

The amount of analyzed water-soluble ionic mass on the filter (μg per filter) is

$$M_{IC} = \Sigma (m_{\text{ppm},j} - m_{\text{ppm\_b},j}) V_l, \quad (7)$$

where $m_{\text{ppm},j}$ is the concentration of ion j in a sample extract solution in units of ppm (μg mL^{-1}), $m_{\text{ppm\_b},j}$ is the concentration of ion j in a blank extract solution, and V_l is the extraction liquid volume.

The relative uncertainty of M_{IC}, δM_{IC}, was estimated from

$$\delta M_{IC} = \frac{\Delta M_{IC}}{M_{IC}} = \left[\left(\frac{\Delta m_{IC}}{m_{IC}}\right)^2 + \left(\frac{\Delta V_a}{V_a}\right)^2\right]^{\frac{1}{2}}, \quad (8)$$

where

$$\frac{\Delta m_{IC}}{m_{IC}} = \left[\left(\frac{\left(\Sigma (\Delta m_{\text{ppm},j})^2 + \Sigma (\Delta m_{\text{ppm\_b},j})^2\right)^{\frac{1}{2}}}{\Sigma (m_{\text{ppm},j} - m_{\text{ppm\_b},j})}\right)^2 + \left(\frac{\Delta V_l}{V_l}\right)^2\right]^{\frac{1}{2}}. \quad (9)$$

The uncertainty of individual ionic chemical components (e.g., nss sulfate aerosol) was calculated using (6) through (9) considering only the mass of the individual component.

2.5.3. Uncertainty of calculated submicron aerosol water mass. The water mass concentration, M_w, in μg m^{-3} associated with the submicron aerosol at 33% RH is

$$M_w = \frac{m_w}{V_a}, \quad (10)$$

where m_w is the water mass in units of μg per filter. The relative uncertainty in M_w, δM_w, was calculated from

$$\delta M_w = \frac{\Delta M_w}{M_w} = \left[\left(\frac{\Delta m_w}{m_w}\right)^2 + \left(\frac{\Delta V_a}{V_a}\right)^2\right]^{\frac{1}{2}}, \quad (11)$$

where

$$\Delta m_w = \left[(\Delta m_{\text{chem\_comp}})^2 + (\Delta m_{\text{RH\_T}})^2\right]^{\frac{1}{2}}. \quad (12)$$

Equation (12) takes into account the sensitivity of the calculated water to the uncertainty in the measured chemical composition and the glove box RH and temperature assuming that the aerosol is externally mixed.

2.5.4. Uncertainty of submicron residual aerosol mass concentration. The submicron residual mass concentration, M_r, in μg m^{-3} was calculated from

$$M_r = (m_g - m_{IC} - m_w) / V_a. \quad (13)$$

The relative uncertainty in M_r, δM_r, was calculated from

$$\delta M_r = \frac{\Delta M_r}{M_r} = \left[\left(\frac{(\Delta m_g)^2 + (\Delta m_{IC})^2 + (\Delta m_w)^2}{(m_g - m_{IC} - m_w)^2}\right) + \left(\frac{\Delta V_a}{V_a}\right)\right]^{\frac{1}{2}}. \quad (14)$$

This method of determining the residual mass concen-

tration and its uncertainty relies on the assumptions that all errors are random and that contamination of the samples did not occur beyond that accounted for by the storage and transport uncertainties. A positive or negative systematic error would affect the significance of the result. Examples of such errors (which our methods cannot detect or correct) are the well-known positive and negative artifacts associated with the sampling of semivolatile organic species [e.g., *Turpin et al.*, 1994]. Heating the sampled air up to 10°C above the ambient temperature may have led to the loss of a portion of the semivolatile organics and ammonium nitrate from the substrate [*Ayers et al.*, 1999] thereby resulting in a negative artifact. No attempt was made to correct for the artifact, however, since the information to do so was not available. In addition, the remote marine results are sensitive to the contamination of relatively few samples since absolute residual mass concentrations are small and often not statistically significant on an individual sample basis.

2.6. Trajectory Calculations and Ancillary Data

Air mass back trajectories for the cruises were calculated twice daily at 0000 and 1200 Greenwich Mean Time (GMT) using the hybrid single-particle Lagrangian integrated trajectory model HY-SPLIT 4 [*Draxler*, 1992]. It is based on wind fields generated by the medium-range forecast model (MRF). Trajectories were terminated at the ship's location at 1000 mbar. Back trajectories for the stations also were calculated twice daily at 0000 and 1200 GMT but were done so with an isentropic transport model [*Harris and Kahl*, 1994]. The model calculates trajectories on isentropic surfaces until the specified surface descends to within 100 m of the ground. At this point, the model switches to a layer-averaged mode where an air parcel is advected by winds averaged through the layer 100–600 m above the surface. Input to the model is furnished by the European Centre for Medium Range Weather Forecasts.

Also measured were the concentration of particles with diameters greater than 15 nm and meteorological parameters including surface temperature, relative humidity, and wind speed and direction. During ACE 1 and CSP, measurements were made of atmospheric ^{222}Rn [*Whittlestone and Zahorowski*, 1998] to aid in the characterization of air mass origin.

3. Results: Pacific and Southern Ocean Aerosol

3.1. Background Information

Measurements were made on four cruises in the Pacific and Southern Oceans between 1993 and 1996 (Figure 1 and Table 1). Data from all cruises were combined and then separated into 20° latitude bins (60–70°S, 40–60°S, 20–40°S, 20°S–0°, 0°–20°N, 20–40°N, 40–60°N). These bins are based on the general synoptic pattern of the central Pacific as described below [*Covert et al.*, 1996; *Quinn et al.*, 1996]. Mean concentrations and absolute uncertainties of the chemical components derived from the dichotomous samplers are given in Table 3. Percentile information (based on the dichotomous sampler for ACE 1 and CSP and the seven-stage impactor for RITS 93 and RITS 94) is shown in Figure 2.

At high latitudes in both the Northern and Southern hemispheres ($\gtrsim$40°) the passage of low-pressure systems occurs every few days. Subsidence of air from above the marine boundary layer (MBL) is associated with the frequent frontal activity resulting in short MBL residence times of <1–3 days for an air parcel and the aerosol that it contains. Here, MBL residence time refers to the length of time an air parcel spends below ~900 mbar prior to being sampled on the ship. Belts of strong high pressure persist in the midlatitudes (~20°–40°) of the Northern and Southern hemispheres. Subsidence followed by transport along the edge of the high-pressure systems results in MBL residence times of ~3–5 days. The location of the ship relative to the high-pressure systems determines the trajectory of the sampled air. The well-developed midlatitude highs lead to a tropical depression between ~20°S and 20°N. Within this belt of low pressure, air flows around the equatorward side of the high-pressure systems resulting in relatively stable MBL trade wind flow and long MBL residence times of up to or more than 7 days.

3.2. Aerosol Chemical Components

3.2.1. Sea salt. The highest concentrations of sea salt were measured at high latitudes in both the Northern and Southern hemispheres (Figure 2a). Concentrations were variable in all latitude bands. The arithmetic mean and standard deviation (1σ) for the 60°–70°S latitude band was 0.91 ± 0.59 μg m^{-3}, for the 40°–60°S band it was 0.65 ± 0.33 μg m^{-3}, and for the 40°–60°N band it was 0.96 ± 0.76 μg m^{-3}. This compares to a mean and standard deviation of 0.44 ± 0.39 μg m^{-3} for the 40°S to 40°N latitude band. Within this low-latitude band, highest concentrations were measured between 0° and 20°N, a region that encompasses the Intertropical Convergence Zone with its generally higher wind speeds.

Submicron sea salt plays an important role in determining aerosol optical properties in remote ocean regions because of its large concentration relative to other chemical components [*Quinn et al.*, 1998; *Quinn and Coffman*, 1999; *Haywood et al.*, 1999]. The incorporation of submicron sea salt into models that estimate aerosol radiative forcing requires a source function for the submicron size range. Historically, sea salt source functions have been based on a log-linear fit to mea-

Table 3. Mean Concentrations and Absolute Uncertainties of Major Aerosol Chemical Components for Pacific Ocean Latitude Bins

	Mean Uncertainty	40°–60°N	20°–40°N	0°–20°N	0°–20°S	20°–40°S	40°–60°S	60°–70°S
NH_4^+/nss $SO_4^=$ molar ratio	mean	1.30	0.74	0.81	0.68	0.60	1.1	0.72
	std dev (1σ)	0.43	0.18	0.11	0.36	0.22	0.35	0.57
nss $SO_4^=$	mean, $\mu g\ m^{-3}$	0.48	0.38	0.50	0.40	0.44	0.13	0.26
	ΔM,[a] $\mu g\ m^{-3}$	0.02	0.01	0.01	0.01	0.01	0.01	0.01
nss SO_4 aerosol[b]	mean, $\mu g\ m^{-3}$	0.58	0.43	0.57	0.52	0.48	0.16	0.28
	ΔM, $\mu g\ m^{-3}$	0.02	0.01	0.02	0.01	0.01	0.004	0.01
Sea salt	mean, $\mu g\ m^{-3}$	0.48	0.11	0.54	0.30	0.23	0.58	0.26
	ΔM, $\mu g\ m^{-3}$	0.02	0.01	0.02	0.02	0.01	0.01	0.01
MSA	mean, $\mu g\ m^{-3}$	0.02	0.02	0.01	0.03	0.03	0.03	0.09
	ΔM, $\mu g\ m^{-3}$	0.005	0.003	0.003	0.003	0.002	0.001	0.004
Other inorganic ions[c]	mean, $\mu g\ m^{-3}$	<0.005	<0.005	<0.005	<0.005	<0.005	0.06	<0.005
	ΔM, $\mu g\ m^{-3}$						0.007	
Residual mass	mean, $\mu g\ m^{-3}$	0.57	0.66	0.41	0.35	0.11	0.23	0.22
	ΔM, $\mu g\ m^{-3}$	0.12	0.10	0.16	0.13	0.08	0.05	0.10
Submicron mass[d]	mean, $\mu g\ m^{-3}$	2.0	1.5	1.8	1.5	1.2	1.1	0.96
	ΔM, $\mu g\ m^{-3}$	0.11	0.10	0.16	0.13	0.08	0.05	0.10
Number of samples	N[e]	3	4	7	14	5	16	3
Residual aerosol	N where δM_r,[f] < 1.0	2	4	3	8	1	9	1
	N where $\delta M_r < 0.5$	2	3	1	4	1	3	1

[a] ΔM is the mean absolute uncertainty for a given latitude bin at the 95% confidence level.

[b] The nss $SO_4^=$ aerosol includes nss $SO_4^=$ ion and associated NH_4^+.

[c] Other inorganic ions include NH_4^+ in excess of an NH_4^+ to nss $SO_4^=$ molar ratio greater than 2, NO_3^-, and non-sea salt K^+, Mg^{+2}, Ca^{+2}, Cl^-, and Br^-.

[d] Aerosol mass in the submicron size range (at 33 ± 3% RH) from the gravimetric analysis.

[e] N is number of samples.

[f] δM_r is relative uncertainty = $\Delta M_r / M_r$ where M_r is the residual mass concentration.

Table 4. Relationship Between Submicron Sea Salt Mass Concentration and Wind Speed for Pacific Ocean Latitude Bins

Latitude Bin	N	Wind Speed, m s^{-1}	r^2	a	b
40°–60°N	6	6.3–15	0.51	0.14	0.18
20°–40°N	10	4.7–12	0.84	0.40	0.01
0°–20°N	20	4.4–14	0.35	0.10	0.20
0°–20°S	71	1.3–10	0.23	0.12	0.18
20°–40°S	18	4.8–14	0.18	0.10	0.13
40°–60°S	32	5.3–14	0.43	0.13	0.16
60°–70°S	13	6.8–14	0.18	0.14	0.18

Shown are results of a log-linear fit of the form $\ln(m_{\text{sea salt}}) = aU + \ln b$, where $m_{\text{sea salt}}$ is the submicron sea salt aerosol mass concentration and U is wind speed. Both parameters were measured at 18 m asl. Also shown is the coefficient of determination, r^2, and the number of observations, N.

sured sea salt mass concentrations, m_{seasalt}, and local wind speed, U, such that

$$\ln(m_{\text{seasalt}}) = aU + \ln(b), \tag{15}$$

where m_{seasalt} is in μg m^{-3} and U is in m s^{-1} [e.g., *Woodcock,* 1953; *Lovett,* 1978). This relationship has been applied to data derived from bulk aerosol samples and to data derived from size segregated samples. Using (15) and data from the seven-stage impactor samples to quantify the relationship for latitude bands within the Pacific yields slope values between 0.10 and 0.14 with the exception of the 20°–40°N Pacific latitude band which has a slope of 0.4 (Table 4). The lower range of values agrees with those previously reported from shipboard measurements in the Pacific (0.16 [*Woodcock,* 1953]), the Atlantic (0.16 [*Lovett,* 1978]), and the North Sea (0.12 [*Marks,* 1990]).

The coefficient of determination, r^2, ranges from 0.18 to 0.84 indicating that 18 to 84% of the variance in the sea salt mass concentration can be explained by the local wind speed. Other factors affecting the submicron sea salt concentration at any point in time include long-range transport, vertical mixing, and dry and wet deposition [*Gong et al.,* 1997; *Quinn et al.,* 1998; *Bates et al.,* 1998]. As a result, an accurate description of the size-dependent concentration of sea salt throughout the boundary layer requires the coupling of the source function in (15) with a chemical transport model.

3.2.2. NSS sulfate aerosol. The latitudinal distribution of submicron nss sulfate aerosol concentrations (Figure 2b) reflects the pattern of anthropogenic SO_2 emissions from the continents [e.g., *Langner and Rodhe,* 1991]. High concentrations were measured in the midlatitudes of the Northern Hemisphere (mean and standard deviation (1σ) of 0.90 ± 0.89 μg m^{-3} between 20° and 40°N) and relatively low concentrations in the midlatitudes and high latitudes of the Southern Hemisphere (0.18 ± 0.07 μg m^{-3} between 40° and 60°S).

Concentrations measured between 40°S and 60°N were highly variable. In the midlatitudes to high latitudes this was due in large part to the position of the ship relative to moving high- and low-pressure systems and hence to exposure to a variety of atmospheric transport pathways. For example, during RITS 93, the ship traveled north through a pseudostationary high between 20° and 40°N. On the equatorward side of the high, the sampled air was transported along the edge of the high from the northeast near North America to the ship. During RITS 94, the ship traveled south within a low-pressure system through the same region. In this case, the sampled air was transported along the edge of the low bringing marine air from the northwest to the ship.

High concentrations were measured between 40° and 60°N along 140° to 160°W during ACE 1 (mean and standard deviation (1σ) of 1.1 ± 0.28 μg m^{-3}) and between 20° and 40°N along 140°W during RITS 93 (1.7 ± 0.87 μg m^{-3}). In both cases, air mass back trajectories indicate that the sampled air masses were advected from North America. Low concentrations were measured in the 40° to 60°N region during RITS 93 and RITS 94 (0.32 ± 0.10 μg m^{-3}) and in the 20° to 40°N region during ACE 1 and RITS 94 (0.33 ± 0.15 μg m^{-3}. In these cases, back trajectories indicate that the sampled air masses originated from the northwest and had spent several days over the ocean prior to reaching the ship.

Volcanic activity also contributed to the observed variability between 40°S and 20°N. The highest value measured in the Pacific (5.2 μg m^{-3}) was during the ACE 1 cruise at 19°N and 156°W as the ship entered the Hawaiian volcano plume. At this same location, particle concentrations rose to 3000 cm^{-3}, and SO_2 concentrations rose to above 1000 pptv (W. De Bruyn, personal communication, 1995). Similarly, a high nss $SO_4^=$ aerosol concentration (1.3 μg m^{-3}) was observed during ACE 1 near 36°S just east of New Zealand. Coincident with the high-nss sulfate aerosol concentration were relatively high particle (1200–2000 cm^{-3}) and Rn^{222} (500–800 mBq^{-3}) concentrations. Back trajectories indicate that the sampled air passed over New Zealand just prior to reaching the ship. The high-nss $SO_4^=$ concentrations could have been due, at least in part, to the volcanic activity of Mount Ruapehu which is located in the center of the North Island.

3.2.3. Methanesulfonate. The latitudinal distribution of MSA is shown in Figure 2c. Highest concentrations were measured in the 60°–70°S latitude band. Within this latitude band, concentrations were higher during austral summer (0.18 ± 0.09 μg m^{-3}) than during austral fall (0.03 ± 0.02 μg m^{-3}). This seasonality corresponds to higher ocean biological productivity during the summer and to higher measured concentrations of atmospheric dimethylsulfide, the gas phase precursor of MSA [*Quinn et al.,* 1996].

3.2.4. Other inorganic ions. Concentrations of other nonsea salt inorganic ions were above detection limit only during ACE 1 in the 40°–60°S region. Nonsea

salt Ca^{+2} was the major contributor to this mass fraction. Nonsea salt Ca^{+2} also was observed at Cape Grim during ACE 1 [*Sievering et al.,* 1999], and single particle analysis by scanning electron microscopy/energy dispersive x-ray analysis (SEM/EDXA) indicated that it was not of crustal origin. Ca^{+2} concentrations enriched relative to the composition of seawater have been previously reported for the eastern equatorial Pacific [*Maenhaut et al.,* 1983] and the central equatorial Pacific [*Mouri et al.,* 1993]. It has been hypothesized that divalent cations become concentrated in ocean surface water since they bind more strongly to the organic molecules present in the microlayer than do monovalent cations [*MacIntyre,* 1974; *Maenhaut et al.,* 1983]. Bursting bubbles resulting from wind and wave action inject the surface layer into the atmosphere producing sea salt particles whose composition reflects, at least in part, the surface layer chemical composition.

3.2.5. Residual aerosol. Given the high degree of variability in the calculated residual mass concentrations (Figure 2d), an uncertainty analysis was performed to determine if the mean residual mass concentration within each latitude band was significant relative to the experimental uncertainty. Mean absolute and relative uncertainties at the 95% confidence level resulting from this analysis are reported in Table 3. All latitude bands have significant residual mass given that each has a mean relative uncertainty less than 1.0. The mean relative uncertainties of the latitude bands vary from 15 to 73% with the highest value corresponding to the 20°–40°S region. This result is statistically robust if the assumptions of the uncertainty analysis are valid, i.e., if all errors are random and normally distributed and contamination of the samples did not occur beyond that accounted for by the storage and transport uncertainty. Also listed in Table 3 is the number of samples within each latitude band with a mean relative uncertainty for the residual mass less than 1.0 and less than 0.5. Even though the mean relative uncertainty was less than 0.5 for all latitude bands but one, the relative uncertainty for many of the individual samples within some of the latitude bands was greater than 0.5.

Mean residual mass concentrations were higher in the Northern than the Southern Hemisphere. A relatively high mean residual mass concentration was observed between 40° and 60°N during ACE 1 along 140° and 160°W (mean and standard deviation (1σ) of 0.95 ± 0.24 $\mu g\ m^{-3}$) and was coincident with a high-nss $SO_4^=$ aerosol mean concentration. A high mean value also occurred during RITS 93 in the same latitude band but along 140°W (0.66 ± 0.16 $\mu g\ m^{-3}$). In this case the nss $SO_4^=$ aerosol concentration was low. On the basis of back trajectories and Rn^{222} concentrations, the air mass sampled during ACE 1 was continentally influenced, while that sampled during RITS 93 was of a more marine origin. Hence, residual mass concentrations were found to be relatively high in both continental and marine air masses.

Relatively high residual mass concentrations also were measured in the tropics along 170° and 160°W during CSP and ACE 1, respectively. Trajectories indicate that in both cases, the sampled air arrived from the east in stable trade wind flow and spent up to 1 week or more in the boundary layer prior to arrival at the ship. The longer time spent in the MBL could have allowed for the accumulation of residual mass through vapor deposition and cloud processing.

Previously reported concentrations of carbonaceous aerosol and mineral dust reveal information about the likely chemical composition of the residual mass. Northern Hemisphere mean organic carbon concentrations range from 0.21 to 0.82 $\mu g\ C\ m^{-3}$ [*Chesselet et al.,* 1981; *Barger and Garrett,* 1976; *Andreae et al.,* 1984], while Southern Hemisphere mean concentrations range from 0.11 to 0.22 $\mu g\ C\ m^{-3}$ [*Barger and Garrett,* 1976; *Hoffman and Duce,* 1977; *Cachier et al.,* 1986; *Andreae et al.,* 1984]. Concentrations measured at Cape Grim, Tasmania, which is within the ACE 1 study region, averaged 0.23 ± 0.07 $\mu g\ C\ m^{-3}$ during September of 1979 [*Andreae,* 1982]. Carbon isotope analysis and concentration differences between the hemispheres led *Cachier* [1989] to conclude that much of the organic carbon in the Northern Hemisphere is of anthropogenic origin.

Mineral dust also may be a significant contributor to the residual mass concentration over the Pacific depending on the location and time of year [*Duce,* 1995]. Highest concentrations are reported for the midlatitudes to high latitudes during the spring when dust is transported from Asian desert and loess regions to the mid-Pacific. For example, concentrations at Midway (28°N, 177°W) range from 0.04 $\mu g\ m^{-3}$ during the summer and winter to 7.8 $\mu g\ m^{-3}$ during the spring [*Uematsu et al.,* 1983]. Concentrations are low throughout the equatorial and south central Pacific, although pulses of dust in the equatorial Pacific are not unheard of in the spring [*Uematsu et al.,* 1983; *Prospero et al.,* 1989]. Higher concentrations with a seasonal cycle consistent with transport from Australian dust regions are reported for the western south Pacific near Australia; the mean concentration reported for Norfolk Island (29°S, 167°E) is 0.43 $\mu g\ m^{-3}$ [*Prospero et al.,* 1989]. Lowest concentrations reported for marine regions are for the Antarctic Peninsula (69°S, 61°W) with a mean of 0.0025 $\mu g\ m^{-3}$ [*Dick,* 1991].

The reported concentrations of organic carbon were derived from a number of sampling and analysis methods, all of which are subject to significant artifacts [*McDow and Huntzicker,* 1990; *Hering et al.,* 1990]. The reported mineral dust concentrations and some of the organic carbon concentrations were derived from bulk rather than submicron aerosol samples. In addition, the samples analyzed for carbon and mineral dust were collected at different locations and times than the samples in this study. Given these caveats, it is worth noting that the trend of higher concentrations of carbonaceous and mineral aerosol in the midlatitudes to high lati-

tudes of the Northern Hemisphere and the concentration ranges for the Southern and Northern hemispheres are consistent with the residual mass concentrations reported here.

4. Results: North American Aerosol

4.1. Site Descriptions

Results are presented from four sites in North America which vary widely in their exposure to marine, continental, and polluted air masses.

4.1.1. Barrow, Alaska. Barrow, a polar coastal site, typically is exposed to Arctic haze every year from late winter to early spring as pollutants are transported across the Arctic Basin from Eurasia [*Raatz,* 1989]. During much of the remainder of the year, Barrow is exposed to more southerly flow from the North Pacific or flow from the Arctic Ocean [*Harris and Kahl,* 1994]. For the measurement period presented here (October 1997 to June 1998), Arctic haze influenced the site from the end of December 1997 to the middle of March 1998. This is based on measured nss sulfate aerosol concentrations and aerosol light scattering coefficients. Data are presented for "haze" and "no haze" periods.

4.1.2. Cheeka Peak, Washington. Cheeka Peak, located 3 km from the coast, can be exposed to marine or continental air masses depending on whether the flow is onshore or offshore. Using back trajectories calculated twice daily at 0000 and 1200 GMT [*Harris and Kahl,* 1994], samples were classified as marine or continental. If the trajectory was within the 210°–330° sector for two consecutive days prior to sample collection and the local wind was within the 150°–330° sector, the sample was classified as marine. If the trajectory was within the 330°–150° sector for two consecutive days prior to sample collection and the local wind was within the same sector, the sample was classified as continental. Using these criteria, 11% of the samples collected were classified as marine, and 5% were classified as continental. Only these samples were included in the data analysis. Even among these samples it is difficult to state with certainty that they were purely marine or purely continental. Many of the back trajectories for the marine samples indicate that the sampled air had passed over Alaska three or more days prior to sample collection. Also, it is possible that in some cases the sampled air traveled briefly over Vancouver Island or along the Washington coast prior to sample collection. Likewise, many of the samples classified as continental had passed over the ocean 2–3 days prior to sample collection.

4.1.3. Bondville, Illinois. Bondville is located 13 km southwest of Champaign, Illinois, 250 km northeast of St. Louis, Missouri, 200 km south of Chicago, Illinois, and 180 km west of Indianapolis, Indiana. Hence there are urban areas to the northeast, southwest, north, and east. The site is immediately surrounded by corn and soybean fields. Back trajectories calculated twice daily were used to separate the samples into four categories: from the north (315°–45°), west (240°–315°), south (135°–240°), and east (45°–135°). For a sample to be placed into one of the four categories, the back trajectory had to remain within the same sector three consecutive days prior to sample collection. SO_2 emissions are highest in the southern and eastern sectors with slighty higher emissions during the summer than the other times of the year [*Irving,* 1990]. There also was a seasonal trend in the trajectories during the 1996 and 1997 time period with more trajectories coming from the high-emission southern sector in the spring/summer than in the fall/winter.

4.1.4. Sable Island, Nova Scotia. Sable Island, located 300 km east-southeast of Halifax, Nova Scotia, is exposed to polluted air masses when flow is from North America, clean continental air masses when flow is from the north, and marine air masses when flow is from the Atlantic. Using back trajectories calculated twice daily at 0000 and 1200 GMT [*Harris and Kahl,* 1994] samples were separated into three categories including marine (0°–225°), polluted (225°–300°), and clean continental (300°–0°). For a sample to qualify for a given category, back trajectories had to remain in that sector for three consecutive days prior to sample collection. There were more marine trajectories during the winter and more polluted trajectories during the summer. The occurrence of clean continental trajectories was the same during summer and winter.

4.2. Aerosol Chemical Components

Aerosol chemical component mean concentrations and percentiles are shown in Figure 3 for all four stations. Time series of the chemical component concentrations for Barrow, Sable Island, and Bondville are shown in Figures 4, 5, and 6, respectively. Time series for Cheeka Peak are not shown because of the small sample number. Mean concentrations and absolute uncertainties of the aerosol chemical components are listed in Table 5 for different air mass types at the stations.

4.2.1. Sea salt. Of the four stations, the highest mean concentration of submicron sea salt (mean and standard deviation (1σ) of 1.4 ± 1.3 $\mu g\ m^{-3}$) was measured at Barrow between the end of November and the end of February (Figures 3a and 4a) due to episodically high concentrations. This winter maximum in sea salt concentration agrees with observations from the Canadian Arctic at Alert, Igloolik, and Mould Bay [*Sturges and Barrie,* 1988; *Sirois and Barrie,* 1999]. *Sirois and Barrie* [1999] attributed the maximum to seasonally high winds in the North Atlantic and North Pacific source regions. The mean winter concentration at Barrow is comparable to mean values in the high Southern and Northern Hemisphere latitude bands of the Pacific (see Figure 2a).

The mean sea salt concentration at Barrow for the remainder of the year is comparable to mean marine concentrations measured at Cheeka Peak and Sable Is-

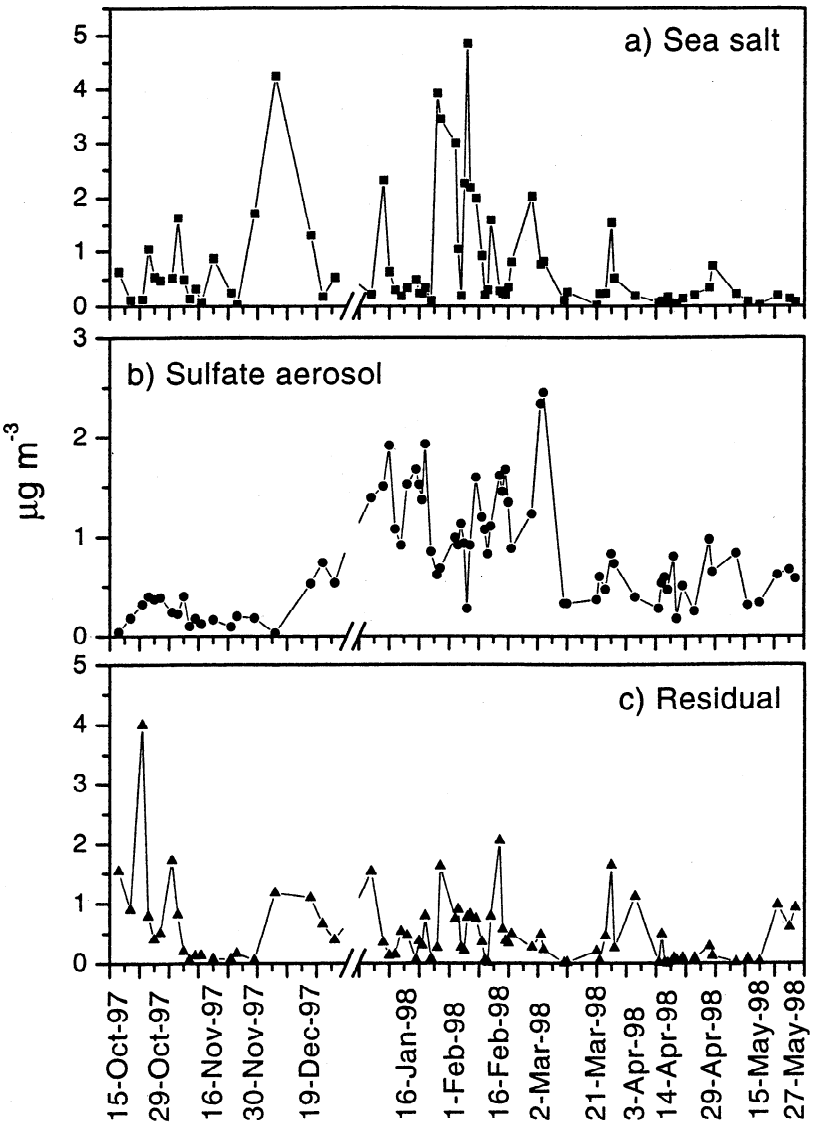

Figure 4. Time series of submicron concentrations of (a) sea salt, (b) nss sulfate aerosol, and (c) residual mass at Barrow.

land. Mean concentrations for samples designated as marine and continental from Cheeka Peak agreed within 10%. This agreement is a function of the site's horizontal and vertical distance from the sea surface, the travel of many of the continental trajectories over the ocean before reaching the site, and the difficulty of collecting a purely marine or continental sample over the one to several day filter sampling period. Mean marine, clean continental, and polluted values at Sable Island agreed within 20% reflecting the fetch over the ocean for any trajectory reaching the site. There was a seasonal trend in the Sable Island values with maximum concentrations occurring in the winter (Figure 5a). This corresponds to more marine trajectories in the winter and to a winter maximum in local wind speed.

4.2.2. NSS sulfate aerosol. Of the four stations, the mean concentration over the entire sampling period was lowest at Barrow and Cheeka Peak. At Barrow, the mean concentration during the Arctic haze season was about twice as high as during the no haze season (mean and standard deviation (1σ) of 1.2 ± 0.54 versus 0.41 ± 0.23 $\mu g\ m^{-3}$) (Figure 4b). The maximum concentration during the haze event was 2.4 $\mu g\ m^{-3}$, and during the no haze period it was 0.97 $\mu g\ m^{-3}$. The strong concentration increase from no haze to haze agrees with previous observations that nss sulfate aerosol is a major component of Arctic haze [*Barrie,* 1986]. It is derived from SO_2 produced in the burning of fossil fuels and smelting of sulfide ores. The concentrations reported here agree well with other measurements that have been made at Barrow. For example, *Shaw* [1985] measured a mean concentration of 1.3 $\mu g\ m^{-3}$ during several late winter/early spring periods between 1976 and 1978, 0.3 $\mu g\ m^{-3}$ during summer, and 0.44 $\mu g\ m^{-3}$ during fall/early

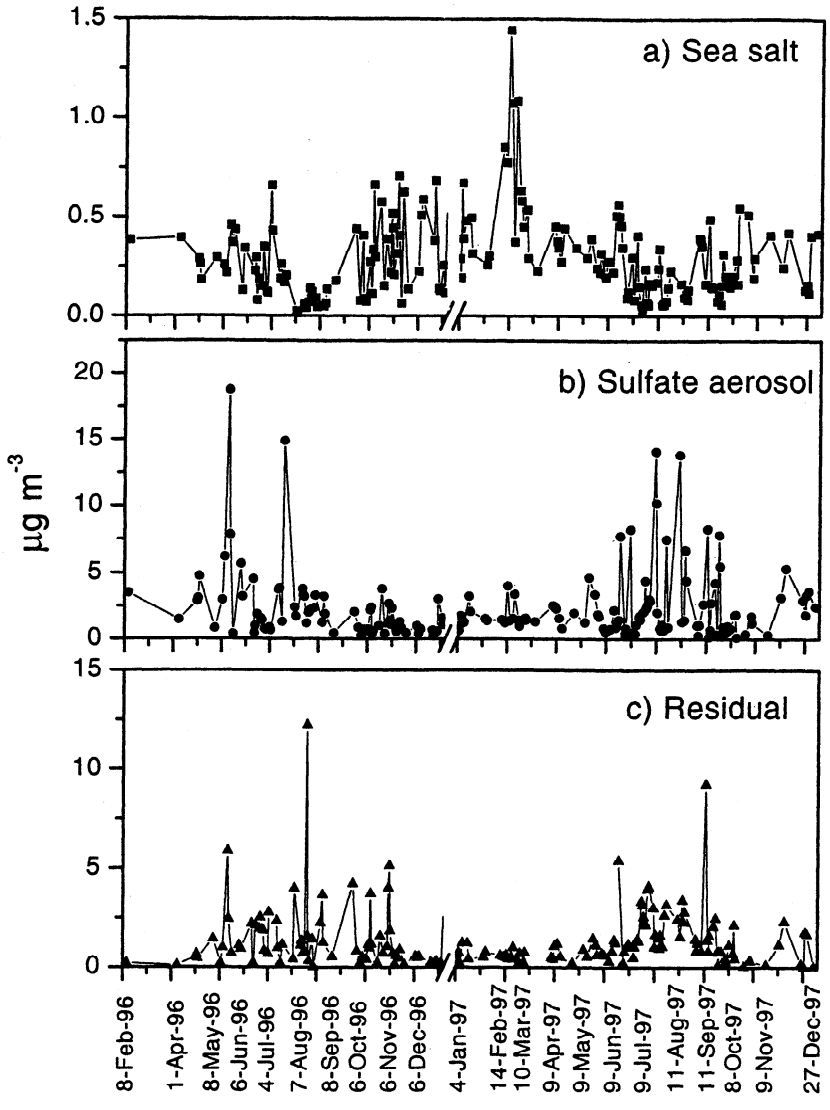

Figure 5. Time series of submicron concentrations of (a) sea salt, (b) nss sulfate aerosol, and (c) residual mass at Sable Island.

winter. *Li and Winchester* [1993] measured a mean submicron concentration of 1.4 μg m^{-3} during March and April of 1989.

The no haze concentrations compare to those for clean marine air masses over the Pacific. This is expected as flow to Barrow during no haze conditions often is from the northeast Pacific [*Harris and Kahl,* 1994]. Haze concentrations are comparable to concentrations of nss sulfate aerosol in continentally influenced Pacific air masses and for marine and continental conditions at Cheeka Peak and Sable Island.

Marine and continental mean concentrations at Cheeka Peak were similar (mean and standard deviation (1σ) of 0.92 $\pm$ 0.56 versus 1.0 $\pm$ 0.28 μg m^{-3}). This, in part, indicates the difficulty of collecting a purely marine or continental sample at Cheeka Peak over the duration of a sampling period. In addition, there are no strong SO_2 sources nearby to elevate the sulfate concentrations in continental air masses. Previously reported values for Cheeka Peak range from 0.2 to 0.7 μg m^{-3} [*Andreae et al.,* 1988; *Bates et al.,* 1990; *Quinn et al.,* 1993]. All of these previous experiments were limited to the April/May time frame which most likely resulted in the observation of lower nss sulfate aerosol concentrations.

The mean concentration at Sable Island during polluted conditions (mean and standard deviation (1σ) of 3.4 $\pm$ 3.2 μg m^{-3}) was about a factor of 3 higher than during marine (1.1 $\pm$ 0.79 μg m^{-3}) and continental (0.93 $\pm$ 0.56 μg m^{-3}) conditions. When flow is from the polluted sector (from the west), Sable Island sits directly downwind of the region of highest SO_2 emissions in the United States [*Irving,* 1990]. In both 1996 and 1997, a seasonal cycle was evident in the nss sulfate aerosol concentrations (Figure 5b) with maximum (although highly variable) concentrations in the summer.

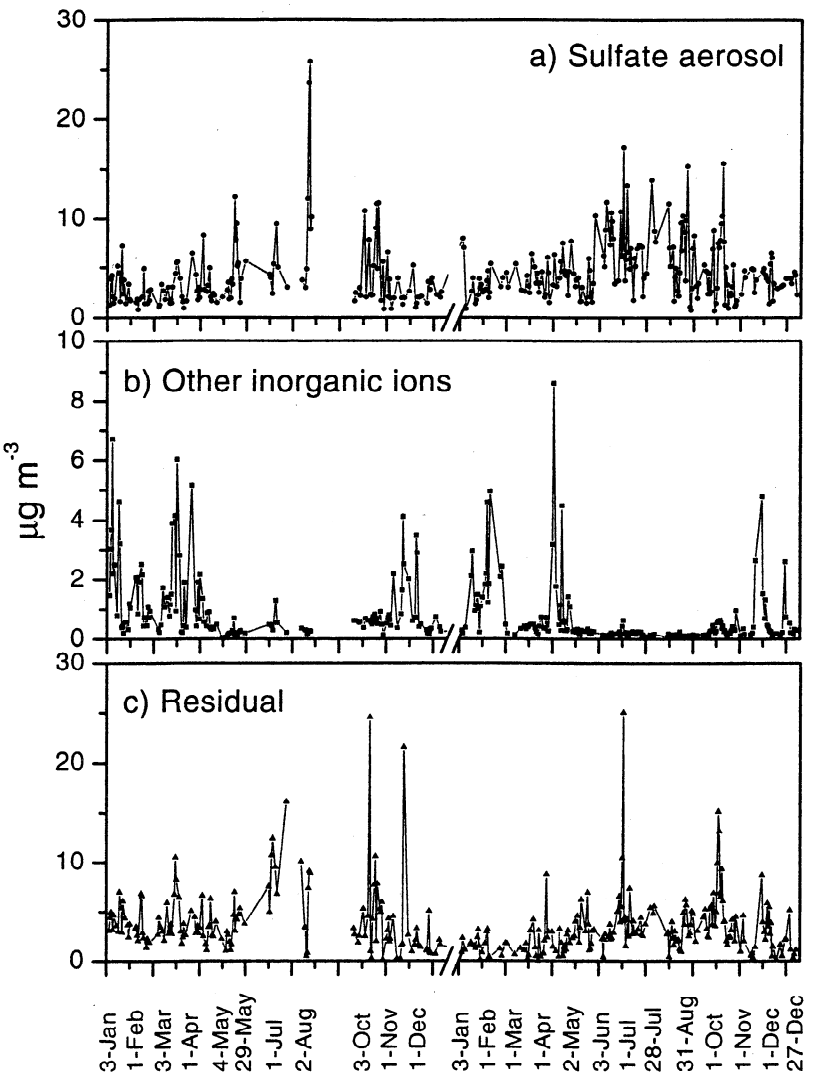

Figure 6. Time series of submicron concentrations of (a) sulfate aerosol, (b) other inorganic ions (not associated with sulfate aerosol), and (c) residual mass at Bondville.

This was due, in part, to the occurrence of more westerly trajectories in the summer than in the other seasons. Higher concentrations of biogenic sulfate aerosol precursor in the summer than the other seasons also may have contributed to the maximum summer concentrations. Considering just marine samples, nss $SO_4^=$ ion concentrations in summer averaged 1.0 ± 0.64 μg m^{-3} while the mean over the rest of the year was 0.47 ± 0.28 μg m^{-3}.

The highest sulfate aerosol concentrations measured at Bondville were associated with trajectories from the east (mean and standard deviation (1σ) of 7.1 ± 2.5 μg m^{-3}) and south (5.8 ± 3.7 μg m^{-3}), regions with large SO_2 emissions (Table 5). The range of concentrations measured during these periods (0.9–26 μg m^{-3}) was similar to the range measured at Sable Island during flow from the west (0.60–19 μg m^{-3}). The median value at Bondville was twice as high, however, 5.2 versus 2.4 μg m^{-3}. Mean concentrations during northerly and westerly flow were the same (3.6 ± 2.9 versus 3.5 ± 2.2 μg m^{-3}) and about a factor of 2 lower than during easterly flow. There was a seasonality to the sulfate aerosol concentrations with maximum values in the summer (Figure 6a). This is due, at least in part, to the occurrence of more southerly trajectories during the summer than other times of the year.

4.2.3. Other inorganic ions. At Barrow the mean concentration of other inorganic ions during Arctic haze was almost a factor of 6 higher than the mean concentration over the rest of the year. The majority of the mass in both cases was NO_3^-. During Arctic haze, NO_3^- concentrations ranged from 0.01 to 1.5 μg m^{-3} and during the rest of the year ranged from the detection limit up to 0.12 μg m^{-3}. Because samples are heated during collection, volatilization of HNO_3 from the sampling substrate could have occurred. Therefore these concentrations represent a lower bound.

Mean concentrations during marine and continental

Table 5. Mean Concentrations and Absolute Uncertainties of Major Aerosol Chemical Components at North American Monitoring Stations

		Barrow		Cheeka Peak		Bondville				Sable Island		
	Mean Uncertainty	Haze	No Haze	Cont	Marine	North	East	South	West	Marine	Clean Cont	Polluted
NH_4^+/nss $SO_4^=$ molar ratio	mean	1.6	1.9	1.5	1.4	1.9	1.8	1.9	2.0	1.2	1.2	1.3
	std dev (1σ)	0.27	0.20	1.1	0.61	0.15	0.17	0.11	0.07	0.29	0.40	0.29
nss $SO_4^=$	mean, $\mu g\ m^{-3}$	0.89	0.31	0.81	0.76	2.6	5.3	4.3	2.5	0.87	0.75	2.7
	ΔM,[a] $\mu g\ m^{-3}$	0.01	0.01	0.02	0.02	0.02	0.12	0.03	0.02	0.01	0.01	0.02
nss SO_4 aerosol[b]	mean, $\mu g\ m^{-3}$	1.2	0.41	1.0	0.92	3.6	7.1	5.8	3.5	1.1	0.93	3.4
	ΔM, $\mu g\ m^{-3}$	0.01	0.01	0.03	0.02	0.02	0.17	0.04	0.03	0.02	0.02	0.03
Sea salt	mean, $\mu g\ m^{-3}$	1.2	0.34	0.29	0.32					0.32	0.29	0.27
	ΔM, $\mu g\ m^{-3}$	0.02	0.01	0.02	0.01					0.01	0.02	0.01
MSA	mean, $\mu g\ m^{-3}$	<0.001	0.001	NA[c]	NA	NA	NA	NA	NA	NA	NA	NA
	ΔM, $\mu g\ m^{-3}$		0.0002	NA	NA	NA	NA	NA	NA	NA	NA	NA
Other inorganic[d] ions	mean, $\mu g\ m^{-3}$	0.23	0.04	0.17	0.10	0.87	0.87	0.48	1.0	<0.005	<0.005	<0.005
	ΔM, $\mu g\ m^{-3}$	0.01	0.02	0.01	0.01	0.01	0.06	0.01	0.02			
Residual mass	mean, $\mu g\ m^{-3}$	0.56	0.49	5.6	0.87	3.1	2.2	4.5	3.0	0.85	0.96	1.6
	ΔM, $\mu g\ m^{-3}$	0.05	0.06	0.27	0.12	0.06	0.32	0.09	0.08	0.07	0.07	0.06
Submicron mass[e]	mean, $\mu g\ m^{-3}$	3.4	1.4	7.6	2.8	8.5	11	12	8.6	2.6	2.5	6.2
	ΔM, $\mu g\ m^{-3}$	0.01	0.05	0.03	0.04	0.01	0.02	0.01	0.01	0.03	0.03	0.01
Number of samples	N[f]	38	39	6	14	141	7	109	68	37	38	100
Residual aerosol	N, δM_r[g] <1.0	24	18	6	10	128	6	104	62	29	29	85
	N, $\delta M_r < 0.5$	14	11	6	2	117	5	101	56	22	21	61

[a] ΔM is the mean absolute uncertainty for a given latitude bin at the 95% confidence level.

[b] The nss $SO_4^=$ aerosol includes nss $SO_4^=$ ion and associated NH_4^+.

[c] NA, no MSA analysis was performed.

[d] For all sites except Bondville other inorganic ions include NH_4^+ in excess of an NH_4^+ to nss $SO_4^=$ molar ratio greater than 2, NO_3^-, and non-sea salt K^+, Mg^{+2}, Ca^{+2}, Cl^-, and Br^-. For Bondville, this includes all measured inorganic ions not associated with sulfate aerosol.

[e] Aerosol mass in the submicron size range (at 33 ± 3% RH) from the gravimetric analysis.

[f] N is the number of samples.

[g] δM_r is relative uncertainty = $\Delta M_r / M_r$ where M_r is the residual mass concentration.

conditions at Cheeka Peak were the same. For samples with appreciable "other inorganic ions" mass, the majority of the mass was excess NH_4^+ meaning NH_4^+ in excess of an NH_4^+ to nss $SO_4^=$ molar ratio of 2. This was the case for both marine and continental. Nitrate concentrations were below the detection limit, suggesting that the excess ammonium was associated with other anionic species such as organic acids. The possibility of sample contamination between collection and analysis cannot be ruled out, but the care with which the samples were handled and the low-NH_4^+ blanks suggest that these values are real.

Mean concentrations of other inorganic ions during northerly, easterly, and westerly flow at Bondville agreed within 15%. The mean during southerly flow was about a factor of 2 lower. The primary inorganic components were NO_3^- and NH_4^+ in excess of an NH_4^+ to $SO_4^=$ molar ratio of 2. Concentrations at Sable Island were below the detection limit.

4.2.4. Residual aerosol. The mean relative uncertainty of the residual mass concentration at each station was 0.14 or less (Table 5), indicating that the calculated residual mass was statistically significant. Of the four sites, the mean residual mass concentration was lowest at Barrow with values for haze and no haze periods agreeing within 15% (mean and standard deviation (1σ) of 0.56 ± 0.47 versus 0.49 ± 0.75 $\mu g\ m^{-3}$). Many measurements of aerosol chemical composition have been made at Barrow during periods of Arctic haze. The reported concentration of mineral dust particles with diameters less than 2.5 μm is 0.9 $\mu g\ m^{-3}$ [*Li and Winchester,* 1990], of black carbon is 0.21 to 0.31 $\mu g\ m^{-3}$ [*Rosen et al.,* 1984; *Clarke,* 1989], and of organic acids in submicron particles is 0.1 $\mu g\ m^{-3}$ [*Li and Winchester,* 1993]. Assuming these species compose the majority of the submicron mass and that half of the mineral dust resides in the submicron size range results in a summed submicron concentration of about 0.8 $\mu g\ m^{-3}$. This falls within the range of calculated residual mass concentrations reported here for Arctic haze conditions. Few chemical measurements have been made during the no haze period, making such a comparison difficult.

At Cheeka Peak the mean residual mass concentration in continental air was about a factor of 6 higher than that in marine air (mean and standard deviation (1σ) of 5.6 ± 0.24 versus 0.87 ± 0.96 $\mu g\ m^{-3}$). One other study has estimated the residual mass concentration at Cheeka Peak. During the Pacific Sulfur Stratus Investigation (PSI-1) conducted in April of 1991, *McInnes et al.* [1996] found that 31–59% of the submicron mass was residual. During the Cloud and Aerosol Chemistry Experiment (CACHE-1) in May of 1993, 50 to greater than 90% of the submicron mass was residual. These values compare well with the mean mass fractions of residual mass found in this study for marine (31%) and continental air masses (74%). *McInnes et al.* [1996] observed that for the very high residual mass cases, individual particle analysis by electron microscopy showed that less than 20% of the total number of particles with diameters between 50 nm and 1.0 μm were sea salt, nss sulfate, or mineral particles. Elemental spectra of the unidentified or "residual" particles contained C, O, and possibly other lower atomic number elements such as N which are not easily identified with an X-ray detector. The particles had a spherical morphology and did not resemble soot, implying that they were of organic composition.

Mean residual mass concentrations measured at Sable Island during marine (mean and standard deviation (1σ) of 0.85 ± 0.66 $\mu g\ m^{-3}$) and continental (0.96 ± 1.0 $\mu g\ m^{-3}$) conditions were within 10% of those measured during marine conditions at Cheeka Peak. The Sable Island marine and continental values were almost a factor of 2 lower than the mean value for polluted conditions (1.6 ± 1.8 $\mu g\ m^{-3}$). The majority of the samples with concentrations greater than 4 $\mu g\ m^{-3}$ corresponded to trajectories from Nova Scotia and New Brunswick. The remainder of the high-concentration samples corresponded to trajectories from the northeast United States. Residual mass had a similar seasonal cycle as nss sulfate aerosol with maximum concentrations in the summer (Figure 5c).

Measurements of aerosol chemical composition were made at Chebogue Point, Nova Scotia (43.75°N, 66.12°W), during the North Atlantic Regional Experiment (NARE) in August and September of 1993 [*Chylek et al.,* 1996; *Liu et al.,* 1996]. Chebogue Point is located 500 km west of Sable Island. The nss sulfate aerosol concentrations measured during the experiment ranged from 0.7 to 14 $\mu g\ m^{-3}$ which agree with the 0.14 to 15 $\mu g\ m^{-3}$ summertime range measured at Sable Island. During both clean continental and polluted conditions, concentrations of water-soluble organics in bulk aerosol samples averaged 0.46 $\mu g\ m^{-3}$ [*Liu et al.,* 1996]. Black carbon, also in bulk samples, averaged 0.07 ± 0.05 and 0.20 ± 0.08 $\mu g\ m^{-3}$ during clean continental and polluted conditions, respectively [*Chylek et al.,* 1996]. The strong correlation of organic carbon mass with the aerosol number concentration below 0.5 μm in diameter indicates that the majority of the carbonaceous aerosol was in the submicron size range. If this is the case, these concentrations of carbonaceous aerosol are consistent with the residual mass concentrations measured at Sable Island.

Bondville had the highest overall mean residual mass concentration of the four sites (Figure 3c). Maximum residual mass concentrations occurred during the summer and fall (Figure 6c). During four 1-week periods in the fall of 1996 and winter of 1997, measurements were made of submicron black and total organic carbon (S. Koloutsou-Vakakis et al., Aerosol properties and radiative forcing at an anthropogenically perturbed midlatitude Northern Hemisphere continental site, submitted

Table 6. Mass Fractions of Aerosol Chemical Components for Pacific Ocean Latitude Bins

	Mean Uncertainty	40°–60°N	20°–40°N	0°–20°N	0°–20°S	20°–40°S	40°–60°S	60°–70°S
nss $SO_4^=$ aerosol[a]	mean	0.30	0.29	0.32	0.34	0.42	0.14	0.29
	ΔMF[b]	0.02	0.02	0.03	0.03	0.03	0.01	0.03
Sea salt	mean	0.24	0.07	0.30	0.20	0.20	0.53	0.27
	ΔMF	0.02	0.01	0.03	0.02	0.02	0.03	0.03
MSA	mean	0.01	0.01	0.01	0.02	0.03	0.03	0.09
	ΔMF	0.003	0.002	0.002	0.003	0.002	0.001	0.010
Other inorganic ions[c]	mean	<0.002	<0.003	<0.003	<0.002	<0.004	0.05	<0.005
	ΔMF						0.01	
Residual mass	mean	0.29	0.45	0.22	0.23	0.09	0.21	0.23
	ΔMF	0.06	0.08	0.09	0.09	0.07	0.05	0.11

The summed mass fraction for each latitude bin is less than 1 as the mass fraction of water associated with the aerosol at 33% RH is not listed.

[a]The nss $SO_4^=$ aerosol includes nss $SO_4^=$ ion and associated NH_4^+.

[b]ΔM_r is uncertainty for a given latitude bin at the 95% confidence level.

[c]Other inorganic ions include NH_4^+ in excess of an NH_4^+ to nss $SO_4^=$ molar ratio greater than 2, NO_3^-, and nonsea salt K^+, Mg^{+2}, Ca^{+2}, Cl^-, and Br^-.

to *Journal of Geophysical Research*, 1998). The mean black carbon concentration was 0.4 ± 0.2 μg C m^{-3} and the mean total organic carbon concentration was 1.7 ± 0.6 μg C m^{-3}. The submicron aerosol mass concentration was 8.4 ± 3.4 μg m^{-3} with 5.3 μg m^{-3} of this being inorganic ions detected by ion chromatography. This leaves 12% of the submicron mass as unknown during this fall/winter period. The remaining unidentified mass could be H, O, or N in the organic material, water associated with the unanalyzed mass, and/or insoluble components.

5. Mass Fractions of the Aerosol Chemical Components

Mass fractions of the aerosol chemical components were calculated from

$$MF_j = \frac{M_j}{M_g} \tag{16}$$

where MF_j is the mass fraction of chemical component j, M_j is the mass of j in μg m^{-3}, and M_g is the submicron aerosol mass in μg m^{-3}. Mass fractions and associated uncertainties at the 95% confidence level for the Pacific and station data are listed in Tables 6 and 7, respectively.

Mean nss sulfate mass fractions for the Pacific Ocean latitude bands ranged from 0.14 to 0.42. The lowest mean value occurred in the 40°–60°S latitude band where nss sulfate aerosol concentrations were low due to the remoteness from continental sources, and sea salt concentrations were relatively high. The highest value occurred in the 20°–40°S region where sea salt and residual mass concentrations were relatively low. Mean sea salt mass fractions ranged from 0.07 to 0.53 and residual mass fractions from 0.09 to 0.45.

Mean mass fractions of nss sulfate aerosol were more variable at the stations than over the Pacific. The lowest mean value of 0.13 occurred at Cheeka Peak during continental conditions due to relatively high residual aerosol concentrations. The highest mean values occurred at Bondville during easterly flow and Sable Island during westerly flow (0.65 and 0.55, respectively). This finding (that sulfate aerosol is the dominant submicron chemical component under polluted conditions in the Midwest and eastern United States) confirms results reported 25 years ago from humidified nephelometry measurements [*Charlson et al.*, 1974a, b].

At Barrow, both sea salt and residual aerosol made up a significant fraction of the submicron aerosol mass. At the other stations, the residual and nss sulfate aerosol were the dominant chemical components. At all stations the relative uncertainty of the residual mass fraction was less than 0.15.

6. Conclusions

The fraction of the submicron aerosol mass due to nss sulfate aerosol was, on average, 0.14–0.34 within 20° zonally averaged latitude bins of the Pacific and Southern Oceans and 0.13–0.65 at the North American midlatitude monitoring stations. Hence a large and variable (both in time and space) fraction of the submicron aerosol was not sulfate. In ocean regions, sea salt mass fractions ranged, on average, from 0.07 to 0.53. The residual, or chemically unanalyzed, mass was found to be significant to the 95% confidence level in all Pacific latitude bands. Mean residual mass frac-

Table 7. Mass Fractions of Aerosol Chemical Components at the North American Monitoring Stations

	Mean Uncertainty	Barrow		Cheeka Peak		Bondville				Sable Island		
		Haze	No Haze	Cont	Marine	North	East	South	West	Marine	Clean Cont	Polluted
nss $SO_4^=$ aerosol[a]	mean	0.34	0.29	0.13	0.33	0.42	0.65	0.48	0.40	0.41	0.37	0.55
	ΔMF[b]	0.004	0.01	0.004	0.008	0.003	0.01	0.003	0.004	0.009	0.009	0.005
Sea salt	mean	0.36	0.24	0.04	0.12					0.12	0.11	0.04
	ΔMF	0.006	0.01	0.002	0.004					0.006	0.006	0.001
MSA	mean	<0.0003	0.0004	NA[d]	NA[d]	NA[d]	NA[d]	NA[d]	NA[d]	NA[d]	NA[d]	NA[d]
	ΔMF		0.0002	NA[d]	NA[d]	NA[d]	NA[d]	NA[d]	NA[d]	NA[d]	NA[d]	NA[d]
Other inorganic ions[c]	mean	0.07	0.03	0.02	0.04	0.10	0.08	0.04	0.12	<0.002	<0.002	<0.003
	ΔMF	0.003	0.011	0.002	0.003	0.001	0.005	0.001	0.002			
Residual mass	mean	0.17	0.34	0.74	0.31	0.37	0.20	0.38	0.35	0.33	0.38	0.26
	ΔMF	0.02	0.05	0.04	0.04	0.01	0.03	0.01	0.01	0.03	0.03	0.01

The summed mass fraction for each station is less than 1 as the mass fraction of water associated with the aerosol at 33% RH is not listed.

[a] The nss $SO_4^=$ aerosol includes nss $SO_4^=$ ion and associated NH_4^+.

[b] ΔMF is uncertainty for a given station at the 95% confidence level.

[c] Other inorganic ions include NH_4^+ in excess of an NH_4^+ to nss $SO_4^=$ molar ratio greater than 2, NO_3^-, and non-sea salt K^+, Mg^{+2}, Ca^{+2}, Cl^-, and Br^-, except for Bondville, where it includes all ions not associated with nss sulfate aerosol.

[d] NA, no MSA analysis was performed.

tions ranged from 0.09 to 0.45. At all of the monitoring stations, the residual mass was significant to the 95% confidence level with mass fractions ranging, on average, from 0.17 to 0.74. The confidence level of 95% relies on the assumptions that all errors were random and normally distributed and that contamination of the samples did not occur beyond that accounted for by the storage and transport uncertainties. In addition, the 95% confidence level only applies to the average of the samples reported here, not to the average aerosol composition within a given latitude bin or at a given station.

The chemical identification of the residual mass is critical to an accurate estimate of aerosol radiative forcing as optical and cloud-nucleating properties depend on chemical composition. A mass closure approach is needed whereby standardized sampling methods are used to determine the aerosol mass and the mass of all chemical components. Agreement between the total mass and the summed mass of the chemical components ensures that all of the aerosol components have been identified. Two additional issues to be resolved are the size distribution of the residual mass and the mixing state of the aerosol chemical components, as these also affect aerosol optical properties.

Acknowledgments. We thank the officers and crew of the now-decommissioned NOAA Research Vessels *Surveyor* and *Discoverer*. In addition, we thank Drew Hamilton, Cyndi Zenker, and Mike Hamilton for analytical assistance. This research was funded by the Aerosol Project of the NOAA Climate and Global Change Program, NOAA's Arctic Research Initiative, and the NASA Global Aerosol Climatology Project. In addition, the work was partially funded by NOAA contract COM NA36GP0300 (MJR). This is NOAA PMEL contribution 2058 and JISAO contribution 705.

References

Andreae, M. O., Marine aerosol chemistry at Cape Grim, Tasmania, and Townsville, Queensland, *J. Geophys. Res., 87,* 8875–8885, 1982.

Andreae, M. O., T. W. Andreae, R. J. Ferek, and H. Raemdonck, Long-range transport of soot carbon in the marine atmosphere, *Sci. Total Environ., 36,* 73–80, 1984.

Andreae, M. O., H. Berresheim, T. W. Andreae, M. A. Kritz, T. S. Bates, and J. T. Merrill, Vertical distribution of dimethylsulfide, sulfur dioxide, aerosol ions, and radon over the northeast Pacific Ocean, *J. Atmos. Chem., 6,* 149–173, 1988.

Ayers, G. P., M. D. Keywood, and J. L. Gras, TEOM vs. manual gravimetric methods for determination of PM2.5 aerosol mass concentrations, *Atmos. Environ., 33,* 3717–3721, 1999.

Barger, W. R., and W. D. Garrett, Surface active organic material in air over the Mediterranean and over the eastern equatorial Pacific, *J. Geophys. Res., 81,* 3151–3157, 1976.

Barrie, L. A., Arctic air pollution: An overview of current knowledge, *Atmos. Environ., 20,* 643–663, 1986.

Bates, T. S., J. E. Johnson, P. K. Quinn, P. D. Goldan,

W. C. Kuster, D. S. Covert, and C. J. Hahn, The biogeochemical sulfur cycle in the marine boundary layer over the northeast Pacific Ocean, *J. Atmos. Chem., 10,* 59–81, 1990.

Bates, T. S., V. N. Kapustin, P. K. Quinn, D. S. Covert, D. J. Coffman, C. Mari, P. A. Durkee, W. DeBruyn, and E. Saltzman, Processes controlling the distribution of aerosol particles in the marine boundary layer during ACE-1, *J. Geophys. Res., 103,* 16,369–16,383, 1998.

Berner, A., C. Lurzer, F. Pohl, O. Preining, and P. Wagner, The size distribution of the urban aerosol in Vienna, *Sci. Total Environ., 13,* 245–261, 1979.

Cachier, H., Isotopic characterization of carbonaceous aerosols, *Aerosol Sci. Technol., 10,* 379–385, 1989.

Cachier, H., P. Buat-Menard, M. Fontugne, and R. Chesselet, Long-range transport of continentally-derived particulate carbon in the marine atmosphere: Evidence from stable carbon isotope studies, *Tellus, Ser. B, 38B,* 161–177, 1986.

Charlson, R. J., A. H. Vanderpol, D. S. Covert, A. P. Waggoner, and N. C. Ahlquist, $H_2SO_4/(NH_4)_2SO_4$ background aerosol: Optical detection in St. Louis region, *Atmos. Environ., 8,* 1257–1267, 1974a.

Charlson, R. J., A. H. Vanderpol, D. S. Covert, A. P. Waggoner, and N. C. Ahlquist, Sulfuric acid-ammonium sulfate aerosol: Optical detection in St. Louis region, *Science, 184,* 156–158, 1974b.

Charlson, R. J., J. Langner, H. Rodhe, C. B. Leovy, and S. G. Warren, Perturbation of the northern hemispheric radiative balance by backscattering from anthropogenic sulfate aerosols, *Tellus, Ser. AB, 43(AB),* 152–163, 1991.

Charlson, R. J., T. L. Anderson, and H. Rodhe, Direct climate forcing by anthropogenic aerosols: quantifying the link between radiation and sulfate models, *Contrib. Atmos. Phys., 72,* 79–94, 1999.

Chesselet, R., M. Fontugne, P. Buat-Menard, U. Ezat, and C. E. Lambert, The origin of particulate organic carbon in the marine atmosphere as indicated by its stable carbon isotopic composition, *Geophys. Res. Lett., 8,* 345–348, 1981.

Chylek, P., C. M. Banic, B. Johnson, P. A. Damianò, G. A. Isaac, W. R. Leaitch, P. S. K. Liu, F. S. Boudala, B. Winter, and D. Ngo, Black carbon: Atmospheric concentrations and cloud water content measurements over southern Nova Scotia, *J. Geophys. Res., 101,* 29,105–29,110, 1996.

Clarke, A. D., Aerosol light absorption by soot in remote environments, *Aerosol. Sci. Tech., 10,* 161–171, 1989.

Covert, D. S., V. N. Kapustin, T. S. Bates, and P. K. Quinn, Physical properties of marine boundary layer aerosol particles of the mid-Pacific in relation to sources and meteorological transport, *J. Geophys. Res., 101,* 6919–6930, 1996.

Dick, A. L., Concentration and sources of metals in the Antarctic Peninsula aerosol, *Geochim. Cosmochim. Acta, 55,* 1827–1836, 1991.

Draxler, R. R., Hybrid Single-Particle Lagrangian Integrated Trajectories (HY-SPLIT): Version 3.0. User's Guide and Model Description, *Tech. Rep. ERL ARL-195,* Natl. Oceanic Atmos. Admin., Silver Spring, Md., 1992.

Duce, R. A., Sources, distributions, and fluxes of mineral aerosols, and their relationship to climate in *Aerosol Forcing of Climate,* edited by R. J. Charlson and J. Heintzenberg, pp. 43–69, John Wiley, New York, 1995.

Gong, S. L., L. A. Barrie, and J.-P. Blanchet, Modeling sea-salt aerosols in the atmosphere 1. Model development, *J. Geophys. Res., 102,* 3805–3818, 1997.

Harris, J. M., and J. D. W. Kahl, Analysis of 10-day isentropic flow patterns for Barrow, Alaska: 1985–1992, *J. Geophys. Res., 99,* 25,845–25,855, 1994.

Haywood, J. M., D. L. Roberts, A. Slingo, J. M. Edwards, and D. P. Shine, General circulation model calculations of the direct radiative forcing by anthropogenic sulfate and fossil-fuel soot aerosol, *J. Clim., 10,* 1562–1577, 1997.

Haywood, J. M., V. Ramaswamy, and B. J. Soden, Tropospheric aerosol climate forcing in clear-sky satellite observations over the oceans, *Science, 283,* 1299–1303, 1999.

Hering, S. V., et al., Comparison of sampling methods for carbonaceous aerosols in ambient air, *Aerosol. Sci. Technol., 12,* 200–213, 1990.

Hoffman, E. J., and R. A. Duce, Organic carbon in marine atmospheric particulate matter: Concentration and particle size distribution, *Geophys. Res. Lett., 4,* 449–452, 1977.

Intergovernmental Panel on Climate Change (IPCC), *Climate Change 1995,* edited by J. T. Houghton et al., Cambridge Univ. Press, New York, 1996.

Irving, P. (Ed.), *Acidic Deposition: State of Science and Technology,* vol. 1, *Emissions, Atmospheric Processes, and Deposition,* U.S. Natl. Acid Precip. Assess. Program (NAPAP), Washington, D.C., 1990.

Koloutsou-Vakakis, S., and M.J. Rood, The $(NH_4)_2SO_4$-Na_2SO_4-H_2O) system: Comparison of deliquescence humidities measured in the field and estimated from laboratory and thermodynamic modeling, *Tellus, Ser. B., 46B,* 1–15, 1994.

Langner, J., and H. Rodhe, A global three-dimensional model of the tropospheric sulfur cycle, *J. Atmos. Chem., 13,* 225–263, 1991.

Li, S. M., and J. W. Winchester, Haze and other aerosol components in late winter Arctic Alaska, 1986, *J. Geophys. Res., 95,* 1797–1810, 1990.

Li, S. M., and J. W. Winchester, Water soluble organic constituents in Arctic aerosols and snow pack, *Geophys. Res. Lett., 20,* 45–48, 1993.

Liu, P. S. K., W. R. Leaitch, C. M. Banic, S.-M. Li, D. Ngo, and W. J. Megaw, Aerosol observations at Chebogue Point during the 1993 North Atlantic Regional Experiment: Relationships among cloud condensation nuclei, size distribution, and chemistry, *J. Geophys. Res., 101,* 28,971–28,990, 1996.

Lovett, R. F., Quantitative measurement of airborne sea-salt in the North Atlantic, *Tellus, 30,* 358–363, 1978.

MacIntyre, F., Chemical fractionation and sea-surface microlayer processes, *Sea, 5,* 245–299, 1974.

Maenhaut, W., H. Raemdonck, A. Selen, R. V. Grieken, and J. W. Winchester, Characterization of the atmospheric aerosol over the eastern equatorial Pacific, *J. Geophys. Res., 88,* 5353–5364, 1983.

Marks, R., Preliminary investigation on the influence of rain on the production, concentration, and vertical distribution of sea salt aerosol, *J. Geophys. Res., 95,* 22,299–22,304, 1990.

McDow, S. R., and J. J. Huntzicker, Vapor adsorption in the sampling of organic aerosol: Face velocity effects, *Atmos. Environ., Part A, 24A,* 2563–2571, 1990.

McInnes, L. M., P. K. Quinn, D. S. Covert, and T. L. Anderson, Gravimetric analysis, ionic composition, and associated water mass of the marine aerosol, *Atmos. Environ., 30,* 869–884, 1996.

Mouri, J., K. Okada, and K. Shigehara, Variation of Mg, S, K, and Ca contents in individual sea salt particles, *Tellus, Ser. B, 45B,* 80–85, 1993.

Myhre, G., F. Stordal, K. Restad, and I. Isaksen, Estimation of the direct radiative forcing due to sulfate and soot aerosols, *Tellus, Ser. B, 50B,* 463–477, 1998.

Prospero, J. M., M. Uematsu, and D. L. Savoie, Mineral aerosol transport to the Pacific Ocean, in *Chemical Oceanography,* vol. 10, edited by J. P. Riley et al., pp. 188–218, Academic, San Diego, Calif., 1989.

Quinn, P. K., and D. J. Coffman, Local closure during ACE 1: Aerosol mass concentration and scattering and backscattering coefficients, *J. Geophys. Res., 103,* 16,575–16,596, 1998.

Quinn, P. K., and D. J. Coffman, Comment on "Contribution of different aerosol species to the global aerosol extinction optical thickness: Estimates from model results" by Tegen et al., *J. Geophys. Res., 104,* 4241–4248, 1999.

Quinn, P. K., D. S. Covert, T. S. Bates, V. N. Kapustin, D. C. Ramsey-Bell, and L. M. McInnes, Dimethylsulfide/cloud condensation nuclei/climate system: Relevant size-resolved measurements of the chemical and physical properties of atmospheric aerosol particles, *J. Geophys. Res., 98,* 10,411–10,427, 1993.

Quinn, P. K., V. N. Kapustin, T. S. Bates, and D. S. Covert, Chemical and optical properties of marine boundary layer aerosol particles of the mid-Pacific in relation to sources and meteorological transport, *J. Geophys. Res., 101,* 6931–6951, 1996.

Quinn, P. K., D. J. Coffman, V. N. Kapustin, T. S. Bates, and D. S. Covert, Aerosol optical properties in the marine boundary layer during ACE 1 and the underlying chemical and physical aerosol properties, *J. Geophys. Res., 103,* 16,547–16,563, 1998.

Raatz, W. E., An anticyclonic point of view on low-level tropospheric long-range transport, *Atmos. Environ., 23,* 2501–2504, 1989.

Rosen, H., A. D. A. Hansen, and T. Novakov, Role of graphitic carbon particles in radiative transfer in the Arctic haze, *Sci. Total Environ., 36,* 103–110, 1984.

Shaw, G. E., Aerosol measurements in Central Alaska, 1982–1984, *Atmos. Environ., 19,* 2025–2031, 1985.

Sievering, H., B. Lerner, J. Slavich, J. Anderson, M. Posfai, and J. Cainey, O_3 oxidation in sea-salt aerosol water: The size distribution of non-sea salt sulfate during ACE-1, *J. Geophys. Res., 104,* 21,707–21,717, 1999.

Sirois, A., and L. A. Barrie, Arctic lower tropospheric aerosol trends and composition at Alert, Canada: 1980–1995, *J. Geophys. Res., 104,* 11,599–11,618, 1999.

Sturges, W. T., and L. A. Barrie, Chlorine, bromine, and iodine in Arctic aerosols, *Atmos. Environ., 22,* 1179–1194, 1988.

Tang, I. N., A. C. Tridico, and K. H. Fung, Thermodynamic and optical properties of sea-salt aerosols, *J. Geophys. Res., 102,* 23,269–23,275, 1997.

Taylor, B. N., and C. E. Kuyatt, *Guidelines for Evaluating and Expressing the Uncertainty of NIST Measurement Results,* NIST Tech. Note 1297, Natl. Inst. of Stand. and Technol., Gaithersburg, Md., 1994.

Tegen, I., P. Hollrig, M. Chin, I. Fung, D. Jacob, and J. Penner, Contribution of different aerosol species to the global extinction optical thickness: Estimates from model results, *J. Geophys. Res., 102,* 23,895–23,915, 1997.

Turpin, B. J., J. J. Huntzicker, and S. V. Hering, Investigation of organic aerosol sampling artifacts in the Los Angeles Base, *Atmos. Environ., 28,* 3061–3071, 1994.

Uematsu, M., R. A. Duce, J. M. Prospero, L. Chen, J. T. Merrill, and R. L. McDonald, Transport of mineral aerosol over the North Pacific Ocean, *J. Geophys. Res., 88,* 5343–5352, 1983.

Whittlestone, S., and W. Zahorowski, Baseline radon detectors for shipboard use: Development and deployment in the First Aerosol Characterization Experiment (ACE 1), *J. Geophys. Res., 103,* 16,743–16,751, 1998.

Wilson, E. B., *An Introduction to Scientific Research,* 272 pp., McGraw-Hill, New York, 1952.

Woodcock, A. H., Salt nuclei in marine air as a function of altitude and wind force, *J. Meteorol., 10,* 362–371, 1953.

Young, J. F., Humidity control in the laboratory using salt-solutions—A review, *J. Appl. Chem., 17,* 241–245, 1967.

T. L. Anderson and D. S. Covert, Box 351640, Department of Atmospheric Sciences, University of Washington, Seattle, WA 98195.

T. S. Bates, D. J. Coffman, J. E. Johnson, T. L. Miller, and P. K. Quinn, NOAA Pacific Marine Environmental Laboratory, 7600 Sand Point Way NE, Seattle, WA 98115. (quinn@pmel.noaa.gov)

G. Forbes, 45 Alderney Dr., Environment Canada, Sable Island, NS, Canada, B2Y 2N6.

J. M. Harris and J. A. Ogren, 325 Broadway R/CMDL, NOAA Climate Monitoring and Diagnostics Laboratory, Boulder, CO 80303.

M. J. Rood, 205 N. Matthews Ave., Department of Civil and Environmental Engineering, University of Illinois, Urbana-Champaign, IL 61801.

(Received July 15, 1999; revised September 7, 1999; accepted October 11, 1999.)